Recent Advances in Metal-Organic Frameworks as Anticancer Drug Delivery Systems: A Review

Abdollah Karami, Omnia Mohamed, Ahmed Ahmed, Ghaleb A. Husseini and Rana Sabouni,*

Department of Chemical Engineering, American University of Sharjah, Sharjah26666, United Arab Emirates

Abstract: Background: Metal-organic frameworks (MOFs), as attractive hybrid crystalline porous materials, are being increasingly investigated in biomedical applications owing to their exceptional properties, including high porosity, ultrahigh surface areas, tailorable composition and structure, and tunability and surface functionality. Of interest, in this review, is the design and development of MOF-based drug delivery systems (DDSs) that have excellent biocompatibility, good stability under physiological conditions, high drug loading capacity, and controlled/targeted drug release.

Objective: This review highlights the latest advances in MOFs as anticancer drug delivery systems (DDSs) along with insights on their design, fabrication, and performance under different stimuli that are either internal or external. The synthesis methods of MOFs, along with their advantages and disadvantages, are briefly discussed. The emergence of multifunctional MOF-based theranostic platforms is also discussed. Finally, the future challenges facing the developments of MOFs in the field of drug delivery are discussed.

Methods: The review was prepared by carrying out a comprehensive literature survey using relevant work published in various scientific databases.

Results: Novel MOFs in biomedical applications, especially in drug delivery, have shown great potential. MOF-based DDSs can be classified into normal (non-controllable) DDSs, stimuli-responsive DDSs, and theranostic platforms. The normal DDSs are pristine MOFs loaded with MOFs and offer little to no control over drug delivery. Stimuli-responsive DDSs offer better spatiotemporal control over the drug release by responding to either endogenous (pH, redox, ions, ATP) or exogenous stimuli (light, magnetism, US, pressure, temperature). The theranostic platforms combine stimuli-responsive drug delivery with diagnostic imaging functionality, paving the road for imaging-guided drug delivery.

Conclusion: This review presented a summary of the various methods utilized in MOF's synthesis along with the advantages and disadvantages of each method. Furthermore, the review highlighted and discussed the latest developments in the field of MOF-based DDSs and theranostic platforms. The review is focused on the characteristics of MOF-based DDSs, the encapsulation of different anticancer drugs as well as their stimuli-responsive release.

1. INTRODUCTION

Cancer remains one of the deadliest known diseases in human history. It presents a significant health hazard at a global level, threatening both developed and undeveloped countries [1]. There are many types of cancer treatments, including surgical intervention,

radiotherapy, chemotherapy [2], and often combined treatments are required to cure or control various cancers. Among treatments for malignancies, chemotherapy emerged as one of the most widely used, as some cancer tumors are challenging to resect, or they may become immune to radiotherapy [3]. However, the toxicity of chemotherapy lies in the fact that it is a non-targeted treatment method, causing severe side effects, such as nausea, vomiting, hair loss, acute cholinergic gastrointestinal effects, heart problems (cardiotoxicity), *etc* [4]. This treatment, which is not able to discriminate between healthy and diseased cells, has paved the way for the development of novel drug carriers.

Traditionally, drug delivery methods are based on two types of carries, organic or inorganic. Organic carriers, such as liposomes, micelles, and polymersomes, are used to encapsulate the therapeutics drug [5-7]. They offer biocompatibility, biodegradability and can be modified chemically to improve their release properties and increase their accumulation at the tumor site [8]. However, these carriers suffer from uncontrolled release due to the lack of well-defined porosity and weak interaction with the drug [9]. The second type of nanovehicles, *i.e.*, inorganic carriers, such as iron oxide nanoparticle (NPs), carbon nanotubes, quantum dots, *etc*., are either conjugated to the therapeutic molecules or offer a large surface area for the agent to adsorb (and hence encapsulate) [10-12]. The major drawback of these carriers is low biocompatibility (*i.e.*, high immunogenicity) [10, 13]. Thus, there is an urgent need to develop an alternative, safer, and more efficient drug carrier type.

Metal-organic frameworks have emerged as hybrid organic/inorganic porous materials that opened the door for numerous biomedical applications (e.g., drug delivery, biosensing, bioimaging, and their use as antimicrobial agents) [14-18]. The crystalline construction of MOFs offers an open porous structure that gives some exceptional and unique properties, such as an extensive high internal surface area (1000 – 7000 m^2/g) [19, 20], high thermal stabilities (ranging from 250 to 500 °C), low density (the lowest density reported is 0.126 g/cm^3) [21], large pore volumes (ranging from 1.1 to 4.4 cm^3/g) [19, 20], permanent porosities, in addition to flexible frameworks that render them more useful compared to other conventional porous solids [22].

"The published manuscript is available at EurekaSelect via https://doi.org/10.2174/1871520621666210119093844."

Table 1. Comparison between MOF synthetic methods based on the advantages and disadvantages.

Method	Description	Advantages	Disadvantages	References
Slow diffusion (low evaporation)	Metal salts and organic ligands are mixed with a solvent at room temperature. Then crystal growth takes place with the slow evaporation of the solvent.	• Ambient pressure and tempera-ture. Sometimes low temperature is employed • Suitable when single crystals areneeded for analysis *via* single-crys-tal X-ray diffraction	• A very slow process (time-consuming) • Not suitable for large scale production	[36-40]
Layer-by-layer deposition (self-assembly)	A 2D functionalized organic surface is subjected to sequential immersion into solutions containing the organic ligand and metal ions, which serve as a nucleation site to grow MOF crystals in a step-by-step fashion.	• Possibility to fabricate structuresnot attainable by conventional synthesis methods • Enables the study of the reaction kinetics of the individual steps involved in the synthesis • Allows better control over the growth and morphology of thin MOF films	• Time-consuming • Difficult to implement on a large scale	[41-44]
Solvothermal	The metal salts and organic ligands and the solvent are mixed at an elevated temperature and pressure below the critical conditions in a closed vessel.	• Wide range for operating temper-atures • Easy for industrial scale-up • Temperature control that pro-motes crystal growth	• High energy consumption • Long reaction times • High costs for vessels that can handlehigh temperature and pressure	[45-48]
Microwave-assisted	The method involves heating the reactants and solvent mixture through microwave radiation.	• Rapid and uniform crystalgrowth and yield • Offers more control of particlesize distribution and morphology of crystals	Challenging to implement on a large industrial scale	[49-51]
Sonochemical (Ultrasound)	High-energy ultrasound waves induce a cavitation phenomenon in which the rapid formation and collapse of bubbles produce high temperatures and pressures that drive the reaction and MOFs formation.	• Produces more uniform particlesize distribution and morphology of crystals • Short reaction times • Efficient when nano-scale MOFsare desired	• Not suitable when a single crystal isneeded for analysis • Challenging to implement on a largescale	[51-54]
Electrochemical	The metal is introduced as an electrode that reacts with an organic linker dissolved in an electrolyte solution along with a conducting salt upon applying a voltage or current.	• Offers the advantage of continu-ous production of MOFs • Fast reaction rates	The diffusion of the organic linker and/or conducting salt molecules into the pores of the crystals during crystallization leads to an inferior-quality MOF com-pared to those synthesized with other methods	[51, 55, 56]
Mechanochemical	A solvent-free method, where a mechanical force such as grinding induces a chemical reaction that produces the MOF crystals	• A solvent-free method • Heating and high pressure arenot required • Relatively short reaction times	• Defects (secondary phases) in theformed crystals are usually obtained • Difficult to obtain a distinguishable sin-gle crystal for analysis	[51, 57, 58]

The high surface area and large pore volume of MOFs enable the efficient encapsulation of biomolecules of different sizes, rendering them more attractive for drug delivery applications. Meanwhile, MOFs' tunability in terms of chemical functionalization and particle sizes allowed scientists to design efficient drug delivery systems (DDSs). The chemical functionalization of MOFs enables the design of MOF-based DDSs that offer dual therapeutic and diagnostic modalities [23, 24]. Controlling the size of MOF nanocarriers allows us to utilize the enhanced permeability and retention (EPR) phenomenon in order to increase the concentration of the therapeutic agents in targeted tumor region.

Several reviews about MOFs' application in drug delivery are available in the literature, each with a different approach and perspective. Some reviews broadly discuss the biomedical applications of MOFs, which encompass not only drug delivery, but also bioimaging, biosensing, and biocatalysis [25-28]. Other reviews focus on the synthesis and drug-loading strategies, as well as release efficiencies and mechanisms [2, 29-31]. The present review highlights the recent advancements in the design of novel MOF-based DDSs. Additionally, it aims to critically discuss the classification of MOF-based DDSs, their performance, advantages and disadvantages, their role in future developments in the field of drug delivery, and the challenges facing the design and implementation of MOF-based DDSs. To this end, the review is organized into three sections: a brief introduction to MOFs' synthesis and their applications in biomedicine, MOF-based DDSs, and their classification, and finally, the challenges and future outlook of MOF-based DDSs.

2. METAL-ORGANIC FRAMEWORKS (MOFS)

The investigation of MOFs as potential drug carriers emerged due to their flexible structure; hence the synthesis process, the pore size, and shape can be designed to accommodate the molecule to be encapsulated in these structures [32]. MOFs also

enjoy other properties that are required for a successful drug delivery system, that include high loading capacity, high chemical and thermal stability, controlled drug release properties, biocompatibility, and ease of surface modification and tunability through a systematic approach to conjugate functional groups and/or change the pore size [33]. In this section, the synthetic routes to produce MOFs will be discussed, along with the strategies to load them for biomedical, specifically, drug delivery applications. Also, some representative examples of various biomedical MOF applications will be highlighted.

2.1. Synthesis of MOFs

There are several methods used for the synthesis of MOFs, each with its advantages and disadvantages. Moreover, when it comes to selecting the synthesis method, several points must be taken into consideration, such as the nature and type of the metal and the organic ligand, the agent/drug to be loaded, the targeted structure and characteristics of the MOF, and their applications [34, 35]. The most common synthesis strategies widely reported in the literature include slow diffusion, solvothermal, microwave-assisted, ultrasound-assisted, electrochemical, self-assembly, and mechanochemical. (Table **1**) presents a summary of these techniques [36-58].

In general, the synthesis of MOFs involves mixing the metalcontaining reactant with the organic compound (linker), either in a solvent or without a solvent (mechanochemical method). The selection of the solvent plays an important role in the reaction (coordination) environment, as the crystals of the MOF are formed in the solvent medium. Thus careful consideration must be taken when selecting the suitable solvent in order to obtain the desired MOF structure [59]. The factors that need to be considered when selecting the appropriate solvent include the solubility of the metal and organic compounds, solvent reactivity, selectivity, polarity, and thermodynamic properties [60]. It is also preferred to select a solvent that has low vapor pressure, is non-toxic, non-flammable, biodegradable, and recyclable [61]. Recently, several new solvents have been used to synthesize MOFs, including ionic liquids, deep eutectic solvents, and surfactants.

In recent years, ionic liquids (ILs) have been investigated in the synthesis of MOFs. ILs are different from typical low-boilingpoint solvents in that they have negligible vapor pressure, are nonflammable, thermally stable, and have high ionic conductivity and polarity that enable them to dissolve metal salts and organic linkers, rendering them potential alternatives to traditional solvents [62, 63]. Also, deep eutectic solvents (DESs) are another possible alternative to conventional solvents. Although DESs have the same physicochemical characteristics as ILs, they are more advantageous than ILs in that they are cheaper, easier to prepare, not affected by the moisture in the air, and eco-friendly [64-66]. In addition, surfactants have been used in the preparation of MOFs. Surfactants are amphiphilic compounds that contain water-soluble (hydrophilic) and oil-soluble (hydrophobic) groups [61]. This remarkable feature enables them to enhance the solubility of both metal salts and organic ligands. Also, surfactant molecules can self-assemble in the reaction media into different aggregates, which can be useful for controlling the size and shape of the MOF's crystal [67]. Moreover, similar to ILs and DESs, surfactants have low vapor pressure and high thermal stability [61].

MOF synthesis and functionalization for biomedical applications, especially drug delivery, faces several challenges, including controlling the pore dimensions and particle size, loading capacity, control over the release of cargo, biocompatibility, and physiological stability [25]. To this end, several strategies to incorporate different molecules such as drugs (or other biomolecules) in MOFs have been implemented, as shown in Fig. (**1**). The surface adsorption, covalent conjugation, and pore encapsulation strategies consist of mixing the synthesized MOF particles with drug-containing solutions. The difference between these strategies manifests in the type of drug-MOF interaction. In surface adsorption (attachment) and pore encapsulation, the dominant interactions are Van der Waals, π-π stacking, and hydrogen bonding, while drug encapsulation *via* covalent conjugation is characterized by chemical bonding between the drug and the MOF [15]. The leading drug-MOF interaction in the *in situ* encapsulation strategy is similar to pore encapsulation, however, the MOF-based nanocarrier's synthesis and drug immobilization take place simultaneously, which is referred to as the one-pot synthesis [15]. Moreover, the biomolecule (e.g., proteins, amino acids, peptides, porphyrins, and cyclodextrins) can be directly incorporated into the MOF as the linker building block in the framework, resulting in a BioMOF [15].

2.2. MOFs for Biomedical Applications

Due to MOFs' unique features, growing efforts have been dedicated to investigating these structures in various biomedical applications such as drug delivery, disease diagnosis, biosensing, and bioimaging. These attractive features include (1) a nanoscale size that enables easier cellular infusion, higher blood circulation

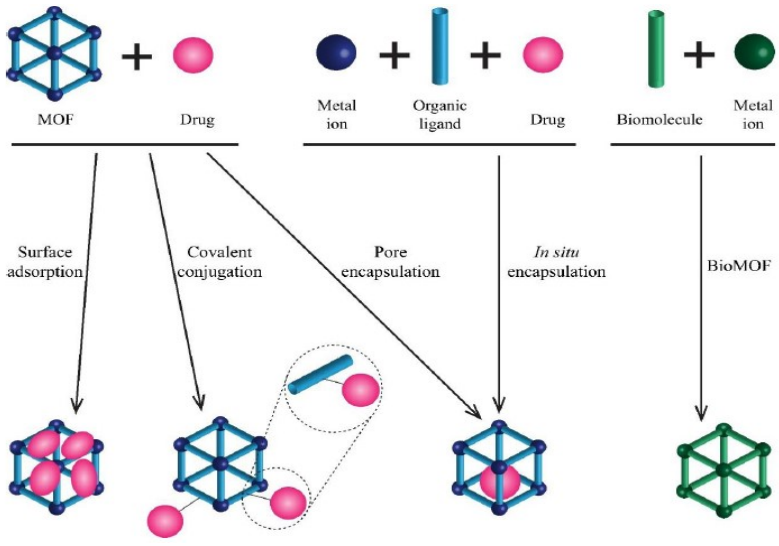

Fig. (1). Schematic representation of the strategies to load drugs into MOFs. (*A higher resolution / colour version of this figure is available in the electronic copy of the article*).

rates, faster kinetics for drug delivery, and being able to utilize the enhanced permeability and retention (EPR) effect [68, 69]; (2) biocompatibility, biodegradability, and chemical stability which means that MOFs can be safely deployed in different biomedical applications because they can be synthesized from biologically-safe metals and organic ligands [69] (BioMOFs can be directly synthesized from biomolecules that are naturally-occurring in the human body; thus they can metabolize safely with little physiological side effects [70]), (3) high and permanent porosity and internal surface area that improve the loading efficiency of different molecules ranging from small to macro sizes [71], (4) easy chemical tuning and functionalization, which make MOFs versatile for a wide range of biomedical applications. Examples related to MOFs and MOF-based composites' potential use in biomedical applications are summarized in (Table **2**) [72-109].

3. MOF-BASED DRUG DELIVERY SYSTEMS (DDSS)

In recent years, the use of MOFs as a drug delivery system (DDS) has seen tremendous developments in terms of features and functionalities, which bodes well for the overall progress in the drug delivery field to achieve enhanced drug loading, faster/controllable release kinetics, and chemical/colloidal stability under physiological conditions. The design of MOF-based DDSs has evolved over the years from normal (non-controllable) to single/multi stimuli-responsive DDS, and more recently into combined therapeutic and diagnostic (theranostic) platforms. This evolution is depicted in Fig. (**2**), which reveals that the classification of the systems depends on their design complexity. As the ability to optimize the design of the DDS in terms of functionality and tuning increases, the complexity of the system increases. On the other hand, the ability to control the drug release in the body also increases, in turn, improving drug delivery to the targeted cells while reducing the potential side effects of the drug. It is always desired to keep the design of the DDS as simple as possible, provided that it serves the requirements in order to scale up the design and deploy it in practical applications. In this section, the different MOF-based DDSs and representative examples of the recent developments in this field are discussed.

Table 2. Examples of MOFs and MOF-based composites used in biomedical applications.

Potential application	Example	Remarks	Reference
Disease diagnosis and drug delivery	UiO-66	UiO-66 was functionalized with polyethylene glycol (PEG). The PEGylated UiO-66 was loaded with dichloroacetic acid (DCA)	[72]
	ZIF-90	ZIF-90 loaded with two anticancer drugs (DOX and 5-FU)	[73]
	NH_2-MIL-101(Fe)	NH_2-MIL-101(Fe) loaded with camptothecin (CAM) and functionalized by folic acid *via* surface modification	[74]
	MIL-100(Fe)	MIL-100(Fe) functionalized with Cyclodextrin (CD) *via* surface anchoring and PEG. The MOF was loaded with azidothymidine (AZT)	[75]
	UiO-Cis	Zr-based UiO MOF with amino-TPDC ligand was loaded with cisplatin and MDR gene-silencing siRNAs for ovarian cancer treatment	[76]
	RIgG@Cu-MOF	Cu-MOF loaded with rabbit antimouse immunoglobulin G antibody (RIgG) for colorimetric immunoassay for antigen mIgG	[77]
	PCN-333	PCN-333 loaded with the enzyme tyrosinase (TYR) for the activation of Paracetamol (APAP) in cancer cells	[78]
	Ni-MOF	A Ni-MOF loaded with Hemin used as an artificial enzyme for the detection of human breast cancer cells (M-CF-7)	[79]
	Cu-TCPP(Fe)	2D Cu-TCPP(Fe)/GOx was constructed by the adsorption of GOx on a 2D Cu-TCPP(Fe) nanosheets for *in vivo* wound healing	[80]
Biosensing	ZIF-8	Glucose oxidase (GOx) and horseradish peroxidase (HRP) enzymes encapsulated in ZIF-8 (GOx&HRP/ZIF-8) for glucose detection	[81]
	ZIF-8 thin film	GOx and HRP enzymes incorporated in a ZIF-8 thin film for glucose detection	[82]
	HP-PCN-224(Fe)	GOx and uricase were immobilized on HP-PCN-224(Fe) to synthesize a mimic multienzyme system that was used for the colorimetric detection of glucose and uric acid	[83]
	Fe-MIL-88B-NH_2	GOx immobilized on Fe-MIL-88B-NH_2 and was used for the colorimetric detection of glucose	[84]
	In-AIP	HRP immobilized on luminescent In-AIP nanosheets and was used for the detection of H_2O_2 and glucose	[85]
	ZIF-8	ZIF-8 loaded with bovine hemoglobin (BHb) using a one-pot synthesis approach. The composite was applied for the detection of H_2O_2	[86]
	AuNP@MIL-101(Cr)	Gold nanoparticles (AuNPs) encapsulated in MIL-101(Cr) to form AuNP@MIL-101(Cr) and then loaded with GOx and LOx. The produced composite was used for the *in vitro* detection of glucose and lactate	[87]
	R-UiO	A dual emissive phosphorescence/fluorescence MOF designed for intracellular O_2 sensing in live cells	[88]
	EAUC	Eu^{3+}/Ag^{+}@UiO-66-$(COOH)_2$ MOF composite for the detection of H_2S as a MOF-based platform for the tentative diagnosis of asthma	[89]
	Zr-MOF	Zirconium-based MOFs were synthesized as platforms for biosensing of lysozyme proteins	[90]

Potential application	Example	Remarks	Reference
Bioimaging	ZIF-90	ZIF-90 loaded with Rhodamine B (RhB) was used for mitochondrial ATP fluorescence imaging in live cells upon the disassembly of the MOF and the release of RhB	[91]
	TP-PCN-58	A Zr-based MOF (PCN-58) covalently modified with two-photon (TP) fluorescent organic probes to add fluorescence-responsive properties to the MOF, which serve to sense and image H_2S and Zn^{2+} in live cells and tissue slices using two-photon microscopy	[92]
	Bi-NU-901	Bismuth NU-901 was tested as an X-ray computed tomography (CT) agent. The MOF was compared with a commercially available CT contrast agent (iodixanol), giving approximately 14 times better contrast than the commercial contrast agent	[93]
	USPIO-MIL-100(Fe)	MIL-100(Fe) MOF coated with maghemite (γ-Fe_2O_3) NPs was used *in vivo* as an efficient magnetic resonance imaging (MRI) contrast agent	[94]
	Gd- BBDC-Glu Yb-BBDC-Glu	Two nanoscale MOF composites synthesized using Gd and Yb as metal nodes, 5-boronobenzene-1,3-dicarboxylic acid (BBDC) as the organic linker and coated with glucose. Gd- BBDC-Glu was used for MRI-guided chemotherapy, while Yb-BBDC-Glu was used for X-ray CT imaging of the gastrointestinal tract.	[95]
	Au@MIL-88(Fe)	Gold nanorods encapsulated in MIL-88(Fe) were constructed for the *in vivo* imaging as imaging nanoprobes in X-ray CT/MRI/PAI systems	[96]
	Fe_3O_4@UiO-66@WP6	Core-shell nanocomposites in which Fe_3O_4 particles are the core and UiO-66 MOFs constitute the shell were constructed, followed by surface coating with carboxylatopillar [6]arene (WP6) that acts as nanovalves and gives the composite multistimuli-responsive release capability. The nanoplatform was used in MRI imaging and MRI-guided cancer therapy.	[97]
	HMONs-PMOF	Hollow mesoporous organosilica NPs combined with polydopamine-MOF. The HMONs-PMOF nanoplatform exhibited dual-modality capacity, which enhanced the MRI and PAI sensitivity.	[98]
	Fe_3O_4@ZIF-8	Fe_3O_4 encapsulated ZIF-8 was utilized as a contrast agent. *In vivo* experiments showed that the composite material displayed contrast enhancement, distinguishing the normal and tumor tissues under MRI.	[99]
Antimicrobial	Ceftazidime@ZIF-8	The antibacterial agent Ceftazidime encapsulated in ZIF-8 MOF showed bactericidal activity against *Escherichia coli* (*E. coli*) upon sustained release of the antibacterial cargo	[100]
	Ag_3(3-phosphonobenzoate)	Silver-based MOFs were tested as bactericidal material against 6 strains of bacteria by utilizing the release of silver ions	[101]
	Cu-BTC	Cu-BTC MOFs showed biocidal activity against fungus and yeast due to the release of copper ions.	[102]
	ZIF-8	A "MOFilter" mask was fabricated as proof of concept by sandwiching ZIF-8 NPs between two non-woven fabric (NWF) layers. The photocatalytic bactericidal performance of the mask was tested by subjecting it to synthetic pathogenic aerosols generated by the *E. coli* suspension. The construct showed a significant drop in the levels of bacteria in the mask in comparison to that of the commercial mask (N95)	[103]
	Vancomycin@MOF-53(Fe)	Antibiotic Vancomycin encapsulated in MOF-53(Fe) showed high antibacterial efficacy against *Staphylococcus aureus* (*S. aureus*)	[104]
	PCN-224-Ag-HA	Antimicrobial nanocomposites were prepared by coating Ag-loaded PCN-224 with hyaluronic acid (HA). These structures showed good biocompatibility with healthy cells while exhibiting an antibacterial effect toward *S. aureus* and MRSA bacteria. The nanoplatform also showed no significant cell cytotoxicity.	[105]
	D-AzAla@MIL-100 (Fe)	3-azido-D-alanine encapsulated in MIL-100(Fe) nanocomposite demonstrated the ability to target the cell walls of methicillin-resistant *S. aureus* (MRSA) bacteria *in vivo*.	[106]
	ZIF-8-PAA-MB@AgNPs@Van-PEG	The composite is constructed by loading ammonium methylbenzene blue (MB) into ZIF-8 MOF functionalized with Polyacrylic acid (PAA), followed by two modifications: Ag NPs and vancomycin/PEG. The material's bactericidal property was demonstrated against three types of bacteria (*E. coli*, *S. aureus,* and MRSA). *In vitro* and *in vivo* experiments were conducted to prove the biocompatibility and antibacterial effect of the composite	[107]
	GS5-CL-Ag@CD-MOF	Ag NPs were embedded in cyclodextrins MOF (CD-MOF) and further functionalized *via* cross-linking with the GRGDS synthetic peptide to produce a nanocomposite named GS5-CL-Ag@CD-MOF. The nanocomposite exhibited a synergistic antibacterial effect and wound healing enhancement	[108]
	PHY@ZIF-8	Physcion (PHY) drug encapsulated in ZIF-8 MOF. The composite exhibited enhanced antibacterial activity in comparison to the pure PHY drug.	[109]

3.1. Normal (non-controllable) MOF-based DDSs

Normal MOF-based DDSs are simply produced by encapsulating the drug molecules into MOF pores *via* the loading strategies discussed in section 2.1. The system delivers the drug with minimum to no stimulus by either disintegrating the MOF structure in the tumor microenvironment (TME) or any other targeted cells, which will provide a burst release or by diffusion (or slow degradation) in which the release profile will be sustained over a longer period. The desired release rate will depend on the nature of the drug and the planned application [110].

Leng and coworkers investigated the loading and release efficiencies of MIL-53(Fe) for the anticancer drug Oridonin (Ori) [111]. The MOF achieved a loading efficiency of 56.25 wt.% and a high release (up to 91.75%) in a 7-day period. Further studies of the cytotoxic effects of Ori-loaded MOFs on HepG2 cells compared to free Ori at the same concentrations showed that Ori-loaded MOFs exhibited the same cell viability as that of the free Ori. In contrast, Ori-loaded MOFs required a more extended period to induce cell death, thus indicating the slow release of the agent from the MOFs and the low cellular uptake.

Also, Lian *et al.* synthesized a PCN-333(Al) MOF from aluminum trimeric clusters and TATB (4,4',4"-s-triazine-2,4,6-triyl-triben-zoicacid) organic ligand using the solvothermal method [112]. The MOF was encapsulated with the tyrosinase (TYR) enzyme as a prodrug Paracetamol (APAP) activator, and the loading efficiency was 80 wt.%. The high loading efficiency could be attributed to the synergistic matching between the MOF's pore size and the TYR size, which also provided good protection from leakage and degradation in the TME. Also, upon the release of TYR, APAP could be activated, which promoted a cytotoxic effect towards the cancer cells through inducing the generation of reactive oxygen species (ROS) and Glutathione (GSH) depletion. The results revealed that the TYR@PCN-333(Al) caused notable tumor regression in the presence of APAP for up to 3 days.

In addition, to prevent the premature drug leakage from the carrier before reaching the diseased cells or to evade the immune system of the body, coating or functionalization of the MOF with other material such as silicon dioxide [113], lipids [114, 115], and exosomes [116] have been reported to improve the performance of MOFs as DDSs. For example, Illes *et al.* investigated the ability of MIL-88A to encapsulate a cocktail of drugs and attempted to control the release by coating the MOFs with a lipid bilayer (liposome) to act as a seal [117]. The loading capacity of MIL-88A with two chemotherapeutic drugs, namely Irinotecan and Floxuridine, was studied individually and as a dual drug mixture. The MOF's individual loading capacity for each drug was 21 and 14.7 wt % for Irinotecan and Floxuridine, respectively. For the mixture of the drugs, a 0.5 mM solution was prepared for each drug and mixed (ratio 1:1) yielding a loading of 10.3 wt % for Irinotecan and 6.9 wt% for Floxuridine (based on UV/Vis measurements). These

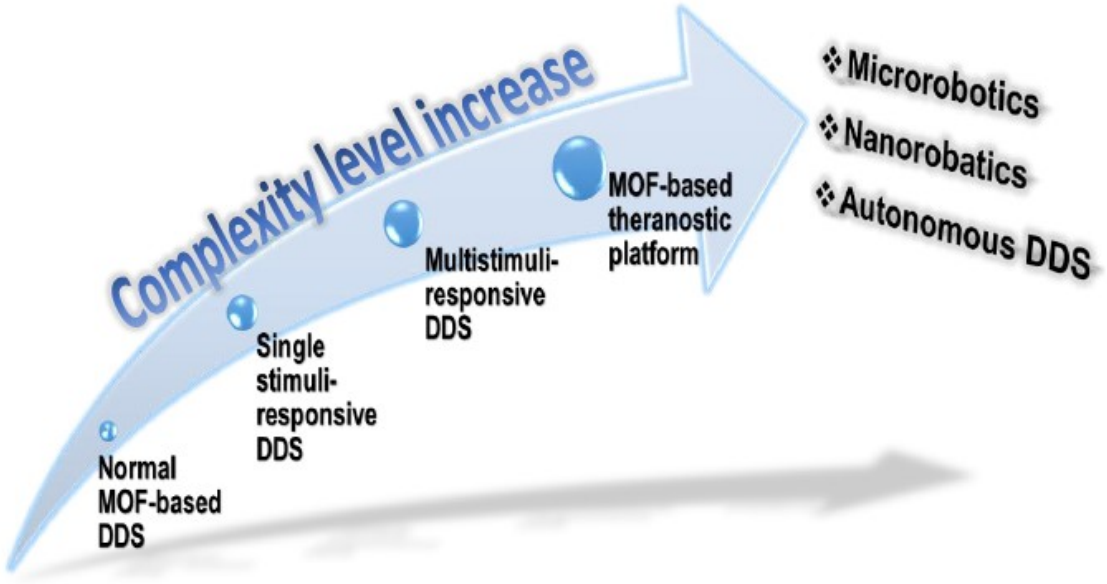

Fig. (2). Developments trend in the MOF-based DDSs. (*A higher resolution / colour version of this figure is available in the electronic copy of the article*).

results confirm the effectiveness of MIL-88A as a promising nanocarrier to deliver a cocktail of drugs. Illes *et al.* further compared the performance of MIL-88A with the coated liposomal MOFs (named Lip-MIL-88A). The MIL-88A was loaded with calcein and incubated for 2 hours in the liposomal solution, DOPC (1,2-dioleoyl- sn-glycero-3-phosphocholine). A sample of the Lip-MIL-88A was used as a test for leakage against uncoated loaded MIL-88A and other samples treated with Triton X-100 and artificial lysosomal fluid (ALF) that induce the rupture of the liposomes coating. The coated MOFs showed no release even after several hours compared to uncoated MOFs that showed a fluorescence increase thus, proving the effectiveness of the liposomes seal. Both the Triton X-100 and ALF treated MOFs showed dramatic release compared to coated untreated MOFs and uncoated MOFs, which is explained by the release of calcein that diffused into the area between the MOFs and the liposomes' inner surface. Cell release experiments were conducted to study the uptake of cells to Lip-MIL-88A by incubating the calcein-loaded nanocarriers with HeLa cells. Lysosomes started breaking up the coated MOF after 2 days and the release of calcein was observed. This established the ability of the hybrid liposomes/MOFs system to exhibit strong drug delivery capability without premature release. Further, single and multidrug MTT assays were conducted for Lip-MIL-88A loaded with irinotecan and floxuridine individually and as a mixture of the two

drugs. Multi-drug loaded Lip-MIL-88A reduced cell viability up to 30.6%, surpassing single drug-loaded carriers.

Furthermore, Wuttke *et al.* studied coating MIL-100(Fe) and MIL-101(Cr) MOFs *via* a lipid bilayer using a controlled solvent deposition exchange procedure [114]. Moreover, fluorescence release experiments were conducted on both calcein-loaded MOF@lipid nanocarriers, and no significant release over a onehour period was observed. In contrast, the addition of Triton X-100 showed a rapid fluorescence increase, which confirmed the bilayer localization on the MOFs' surface. The localization of the lipid bilayer was further explored utilizing a fluorescence confocal microscope. *In vitro* experiments were also conducted to find the cellular uptake of coated MIL-101(Cr) by bladder carcinoma. The cellular uptake was detected within 6 hours and lasted for 48 hours.

In addition, Yang *et al.* focused on resolving the biological instability of Zirconium (Zr) MOFs [115]. The existence of phosphate in most biological systems limited the use of Zr-MOFs as drug carriers due to the high affinity of phosphate-to-metals compared to the organic linker. Consequently, this affinity can induce the substitution of the organic linkers by the phosphate group and result in the collapse of the MOF's structure. In their work, Yang *et al.* reported coating a Zr-based porphyrinic MOF (PCN-223) with DOPC lipids in two stages; the first stage was dissolving the lipids in chloroform then stirring the resultant solution in the presence of the MOF for 24 hours. This resulted in the formation of a monolayer by the attachment of the free oxygen sites on the surface of MOF to the phosphate group of DOPC lipids. In the second stage, DOPC and cholesterol were dissolved in ethanol, and a water solution, followed by the addition of the monolayer coated MOFs and gradual evaporation of the solvents. The presence of the bilayer on PCN-223 was confirmed using several methods including, FTIR, TEM, XRD and DLS. Samples incubated in phosphate-buffered saline (PBS) at pH 7.4 of phospholipid-coated and bare MOFs showed less than 3% degradation after 7 days in PBS for the coated MOFs, compared to the bare MOFs (about 89%). Various solutions of chemicals that nanocarriers can encounter under physiological conditions such as H_2O_2, H_4PDP, and phosphate were exposed to both coated and uncoated MOFs. The bare MOFs showed significant degradation upon exposure to H_2O_2, H_4PDP, and phosphate ions, whereas the coated MOFs showed no significant degradations in all the solutions, establishing the sealing ability and impermeability of the lipid bilayer.

3.2. Stimuli-responsive MOF-based DDSs

As shown in Fig. (**3**), a MOF-based stimuli-responsive DDS is a system that, upon a specific stimulus or a change in the physiological conditions, responds by undergoing a change in their characteristics and/or structure, making it possible for the release of the encapsulated cargo in a temporal, targeted, and dosage-controlled fashion. The changes may or may not be reversible depending on the parameters used in the system. The stimuli can be grouped into two main categories; endogenous (internal), such as pH, redox, ATP, ions, *etc*., or exogenous (external), such as light, heat, electromagnetic, magnetic fields, ultrasound, *etc* [118, 119]. This section discusses the different types of stimuli-responsive MOF-based DDSs, along with some examples. A summary of representative examples of stimuli-responsive MOF-based DDSs and their loading/release efficiencies is presented in (Table **3**) [120-172].

3.2.1. Endogenous Stimuli-responsive Drug Delivery

Endogenous stimuli refer to the differences between the physiological properties of the target diseased cells and the surrounding healthy cells. For example, cancerous cells have a different tumor microenvironment (TME) compared to the surrounding normal cells in terms of pH, redox state, and the nature and amounts of ions (or other biomolecules) [173], and thus these gradients can be exploited as triggers for the targeted release of the encapsulated drug from the DDS against the target cells. However, endogenous stimuli-responsive DDSs may suffer from a low level of flexibility and control, especially when it comes to timely drug delivery since the release of the drug from the DDS will be triggered as soon as it reaches the stimuli-containing target. One approach to resolve this issue is by modifying the MOF's surface by coating with polymers such as polyethylene glycol (PEG) [174], which will extend release time by slowing down the disintegration

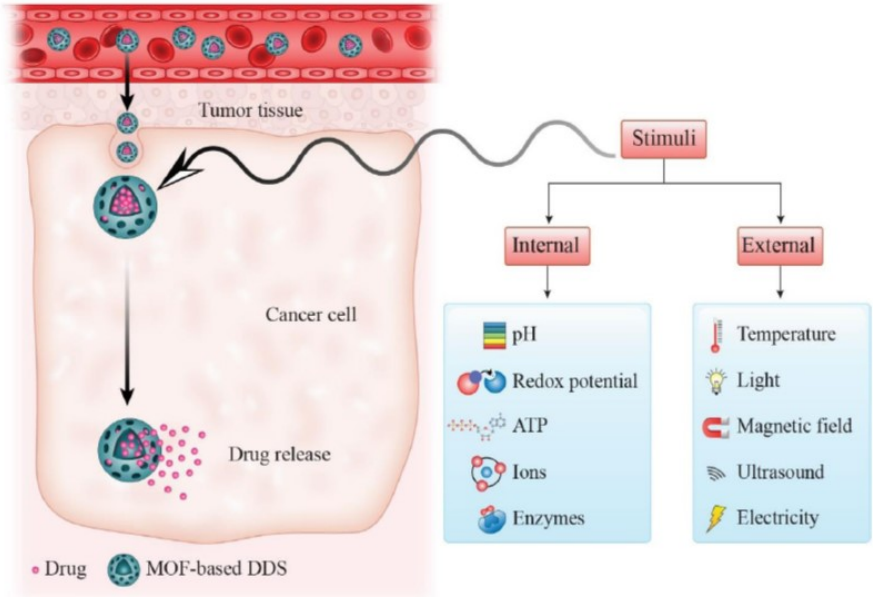

Fig. (3). Schematic illustration of MOF-based stimuli-responsive DDSs. (*A higher resolution / colour version of this figure is available in the electronic copy of the article*).

of the DDS in the physiological environment. Another modification strategy is the functionalization of the MOF with molecules that act as gates, essentially preventing the release of the drug from the DDS until a particular endogenous stimulus such as pH, ATP, enzyme, *etc*. triggers the "unlocking" of the "gate," thus allowing the release of the drug [149, 175].

Table 3. Representative examples of stimuli-responsive MOF-based DDSs and their loading and release efficiencies.

MOF-based DDS	Drug (Cargo)	Loading strategy	Stimuli type	Loading*	Release*	Reference
IRMOF-3@Gel	DOX, CEL	Pore encapsulation	pH	DOX = 46.85 CEL = 26.47	DOX ≈ 80 CEL = 65.77	[120]
CCM@ZIF-L	CCM	*In situ* Encapsulation	pH	98.21	81.2	[121]
DOX@CMC/MOF-5/GO	DOX	Pore encapsulation	pH	6	26	[122]
ZGGO@ZIF-8-DOX	DOX	Surface adsorption	pH	93.2	47.8	[123]
UCNPs@MIL-PEG	DOX	Surface adsorption	pH	60	58	[124]
APT-Mn-ZIF-90	5-FU	Surface adsorption	pH	67.93	90	[125]
FZIF-8/DOX-PD-FA	DOX	Pore encapsulation	pH	258.8 mg/g	57	[126]
Ca/Pt(IV)@pHis-PEG	Pt(IV)	*In situ* Encapsulation	pH	–	95	[127]
Sgc-8 aptamer-PDA-DOX/ZIF-8 FA–PDA–DOX/ZIF-8	DOX	Pore encapsulation	pH	68.78	≈ 100	[128]

MOF-based DDS	Drug (Cargo)	Loading strategy	Stimuli type	Loading*	Release*	Reference
ZnO-DOX@ZIF-8	DOX	*In situ* Encapsulation	pH	11.2	80	[129]
FUGY/DOX	DOX	Surface adsorption	pH	43.8	48.6	[130]
Cu-MOF/MTX@GM	MTX	Pore encapsulation	pH	68	67.52	[131]
5-FU@Dy(III)-MOF	5-FU	Pore encapsulation	pH	20.6	75	[132]
5-FU@ Zn-MOF	5-FU	Pore encapsulation	pH	36.82	86.5	[133]
DOX@ZIF-8@AS1411	DOX	*In situ* Encapsulation	pH	0.1 mg/mg	80	[134]
DOX@ZIF-8/PEG	DOX	*In situ* Encapsulation	pH	10	≈ 100	[135]
BSA/DOX@ZIF-8	DOX	*In situ* Encapsulation	pH	19	80	[136]
$[Zn_2(ad)_2(fmdb)\ (H_2O)](DMF)_3$	5-FU	Pore encapsulation	pH	44.6	76.3	[137]
URODF	DOX	Covalent conjugation	pH	6.0	79.8	[138]
DOX@PCN-224-DNA	DOX	Pore encapsulation	pH	50 μg/mg	45	[139]
5-FU@nano-1	5-FU	Pore encapsulation	pH	34.32	70.1	[140]
PEG-FA/(DOX+VER)@ZIF-8	DOX, VER	*In situ* Encapsulation	pH	DOX = 8.9 VER = 32	DOX = 41.61 VER = 76.48	[141]
Fe/La-MOF@SiO_2-NH_2	DOX	Surface adsorption	pH	150.24 mg/g	95	[142]
ORI@MOF-5	ORI	Pore encapsulation	pH	52.86	87	[143]
DOX@CS/Bio-MOF	DOX	Pore encapsulation	pH	92.5	93	[144]
UiO-66-350-PA-Pt	Cisplatin	Covalent conjugation	Ion (phosphate ions)	25.7	71	[145]
NU-1000	Insulin	Pore encapsulation	Ion (phosphate ions)	40	90	[146]
DOX@MOF-Au-PEG	DOX	Pore encapsulation	Ion (phosphate ions)	247.4 μg/mg	100	[147]
UiO-68/hydrogel	DOX	Pore encapsulation	ATP	79.1 nmol/mg	100	[148]
UiO-68-AS1411	DOX	Pore encapsulation	ATP	46.5 nmol/mg	100	[149]
ZIF-90	Cas9	*In situ* Encapsulation	ATP	> 90	> 90	[150]
DOX@PCN-224-HA	DOX	Pore encapsulation	Redox (Enzyme)	108 mg/mg	–	[151]
HA/α-TOS@ZIF-8	α-TOS	*In situ* Encapsulation	Redox (Enzyme)	43.03	74	[152]
CCM@Zr-DTBA	CCM	Pore encapsulation	Redox (GSH)	78.7	85	[153]
PEGNH_2@5-FU-UiO-AZB	5-FU	Pore encapsulation	Light (UV)	15	–	[154]
AuNR@MOFs@CPT	CPT	Pore encapsulation	Light (NIR)	25.57	30	[155]
(ZIF-8,Tb20)@AuNP	5-FU	Pore encapsulation	Temperature	≈ 27	> 40	[156]
Fe-BTC/MSN@DOX Zn-BTC/MSN@DOX	DOX	*In situ* encapsulation	pH, liposome	80	≈ 100	[157]
ZIF-8@DOX@Organosilica	DOX	*In situ* Encapsulation	pH, redox	41.2	85	[158]
PUWPFa	5-FU	Pore encapsulation	pH, temperature	0.61 μmol/mg	≈ 70	[159]
MTX@ Zn-GA	MTX	*In situ* Encapsulation	pH, temperature	12.85	≈ 100	[160]
5-FU@Zn-cpon-1	5-FU	Pore encapsulation	pH, temperature	44.75	96	[161]
MTX@Zn-TBDA	MTX	*In situ* Encapsulation	pH, temperature	12.59	100	[162]
ICG@ZIF-8-DOX	DOX	Pore encapsulation	pH, NIR	1.71	57	[163]
DOX/Pd@Au@ZIF-8	DOX	*In situ* encapsulation	pH, NIR	39.32 mg/g	70	[164]
H-ZIF-8/PDA-CD	DOX, HCPT	Pore encapsulation	pH, NIR	DOX = 42 HCPT = 9.8	DOX ≈ 86 HCPT ≈ 56	[165]
ZIF-8/GQD	DOX	*In situ* Encapsulation	pH, NIR	47 μg/mg	80	[166]
poly(DH-Se/PEG/PPG urethane)@MOF	DOX	Pore encapsulation	Light, redox	84.2	75	[167]
GSNO/Ce6@ZIF-8@Cytomembrane	GSNO, Ce6	*In situ* encapsulation	pH, US	GSNO = 53.1 Ce6 = 72.8	Ce6 ≈ 80	[168]
CP5-capped UiO-66-NH-Q	5-FU	Pore encapsulation	Zn^{+2}, temperature	115 μmol/g	≈ 70	[169]
CP5-capped UiO-66-NH-A	5-FU	Pore encapsulation	Ca^{+2}, pH, temperature	247 μmol/g	80	[170]
Fe_3O_4@UiO-66@WP6	5-FU	Pore encapsulation	pH, temperature, ions (Ca^{2+}, Zn^{2+})	0.83 μmol/mg	30	[97]
PD/M-NMOF	DOX, MB	*In situ* encapsulation	Magnetism, light	DOX = 0.69 MB = 4.3	DOX = 95 MB = 72	[171]
ZIF-8@ABFs	RhB	*In situ* Encapsulation	pH, magnetism	–	–	[172]

* Unless otherwise stated, the unites of Loading and Release are percent (%)

3.2.1.1. pH-triggered Drug Release

The most common stimulus employed in controlled drug delivery is pH. The pH of human blood is around 7.4, along with most healthy tissues around the body, contrary to the more acidic nature of the extracellular TME, and its intracellular compartments [176]. These pH gradients could be exploited by acting as a trigger for many nanocarriers, including MOF-based DDSs that incorporate pH-sensitive groups in their structure to release their payload [177, 178]. For example, a study by Garcia *et al.* [179], utilized aminofunctionalized MOFs MIL-100 and MIL-101 as a pH-responsive nanoplatform to load the chemotherapeutic drug camptothecin (CPT) by covalent bonding. CPT is a very cytotoxic drug with effective antitumor activity. *In vitro* experiments showed no significant release at physiological pH levels (7.4), compared to a pH level of 5, where the release was highly effective. Also, more recently, Liu *et al.* utilized a water-stable copper-based MOF for the pH-triggered release of 5-Fluorouracil (5-FU) [180]. The synthesized MOF was loaded with the drug 5-FU through surface adsorption and the loading efficiency was 37.22 wt%. The release of the loaded MOF was simulated in PBS at 37 °C at three different pH levels (7.4, 6.8 and 5.8). Experimental results showed that the release at low pH was much more effective than at 7.4. Furthermore, the MTT assay showed that the prepared DDS exhibited no obvious cytotoxicity, was biocompatible, and showed good anticancer activity against A549 and HeLa cell lines.

3.2.1.2. Redox-triggered Drug Release

In recent studies, the redox potential difference between intracellular and extracellular regions has been utilized as a triggering mechanism in stimuli-responsive DDSs. Compared to normal healthy tissues, tumor cells have higher concentrations of glutathione (GSH), which leads to an elevated redox potential in the TME [181]. Intracellular GSH, as a reducing agent, can be oxidized when encountering disulfide bonds, which undergo a rapid bond cleavage [119]. This type of bond could be incorporated in the MOF *via* surface modification to produce a redox-responsive DDS. Upon encountering the high GSH concentration, these disulfide bonds will be cleaved, causing the DDS to disassemble and release the encapsulated drug [181]. Various disulfide bond-containing molecules, *e.g.*, methacrylate-disulfide-camptothecin (CPT), 4,4′-dithiobisbenzoic acid (4,4′-DTBA), and 3,3'-disulfanediyldipropanoyl chloride (DTPC), have been incorporated into MOFs through crosslinking or surface modification [153, 182, 183]. The first attempt to design a redox-responsive MOF-based DDS was reported by Lei *et al.* [153]. The research group developed a novel method to study the effectiveness of a redox stimuli-sensitive MOF in delivering curcumin (CCM) as a chemotherapeutic drug. The MOF was synthesized with zirconium as the metal component and 4,4′-dithiobisbenzoic acid (4,4′-DTBA) as the organic linker. The disulfide bonds in 4,4′-DTBA act as oxidizers to GSH, which is often highly concentrated in the tumor cells. The drug release was tested both *in vitro* and *in vivo*. The redox-responsiveness was tested *in vitro* in PBS containing different concentrations of GSH at pH levels of 7.4 and 5.5. The results showed successful release at both pH levels; however, with increasing concentrations of GSH in PBS, the release of CCM from CCM@MOF-Zr(DTBA) accelerated, indicating the capability of the DDS in stabilizing CCM under normal physiological conditions while being able to release the drug at the tumor site. Also, the *in vivo* antitumor efficiency studies showed a successful reduction in tumor size compared to injecting free CCM. In another study by Xue *et al.* [183], the group designed cubic gel particles (ssCGP) with GSH-responsive features by crosslinking cyclodextrins-based MOF (CD-MOF) templates with DTPC. The DDS exhibited a high loading capacity when loaded with DOX in a period of 40 minutes (45 mg DOX/g DDS). High drug release was achieved in a period of 2 hours in a 100 mM GSH medium.

3.2.1.3. Enzyme-triggered Drug Release

Many enzymes have been recently exploited in MOF-based DDSs as a triggering stimulus, such that the drug will be released upon the disintegration of the enzyme-responsive DDS in the enzyme-rich TME by the redox reaction between the enzyme and the MOF [152]. For example, Sun *et al.* constructed an enzyme-responsive DDS based on ZIF-8 MOF with α-Tocopherol succinate (α-TOS) loading capacity of 43.03 wt.% [152]. The loaded MOF was prepared *via* a one-pot synthetic route and then coated with hyaluronic acid (HA) layer to form the HA/α-TOS@ZIF-8 nanoplatform. The release was achieved through the breakage of the HA layer by hyaluronidase (HAdase) enzymes in the TME, which exposes α-TOS@ZIF-8, hence leading to the disintegration of ZIF-8 to release the encapsulated α-TOS. Similarly, Kim *et al.* reported the release of encapsulated DOX from HA-coated PCN-224 *via* an enzyme-mediated mechanism [151]. The *in vitro* drug release experiment was carried out in an aqueous solution that contained HAdase enzymes, while the control experiment was HAdase free. The results showed that HAdase enzymes degraded the HA layer attached to the PCN-224 surface, leading to drug release. On the other hand, in the absence of HAdase enzymes from the aqueous solution, the HA-coated PCN-224 displayed limited DOX release, suggesting that HA coating provided efficient blocking of DOX premature release.

3.2.1.4. ATP-triggered Drug Release

Another stimulus that can be utilized for the release of drugs is Adenosine triphosphate (ATP), which is a highly active compound that exists in living organisms, acting as a reservoir of energy necessary for many biological processes in a living cell. Usually, ATP is overexpressed in cancerous cells, which can be exploited for the ATP-responsive release of drugs in the targeted cells [184]. For instance, Chen *et al.* prepared a DOX-loaded ATP-responsive DDS by coating UiO-68 with a polyacrylamide hydrogel layer that can degrade by forming an ATP-aptamer complex, which allows the release of the drug [148]. DOX loading was 79.1 nmol/mg, while random leakage was limited to 8%. More recently, Yang *et al.* prepared an ATP-responsive ZIF-90 to deliver Cas9 (a protein used in genome editing) [150]. The DDS encapsulation efficiency was 90%, and the intracellular delivery experiments showed around 90% release of the protein. The DDS was also used to demonstrate the delivery of cytotoxic Ribonuclease A (RNase A), which showed remarkable tumor cell growth inhibition. Moreover, the ATP-mediated release mechanism was determined to be due to the formation of coordination bonds between Zn^{2+} and ATP, leading to breaking the Zn^{2+}/imidazole coordination bond, and hence the disassembly of the MOF.

3.2.1.5. Ions-triggered Drug Release

The presence of ions in the body (e.g., phosphates, calcium, potassium, zinc, *etc*.) can be utilized as bases for the design of ion-responsive DDSs. The ion-triggered release can be achieved by anion exchange with the metal cluster that leads to the breakage of

the MOF structure and the release of the encapsulated drug. Also, the MOF-based DDS can be functionalized with an ion-responsive group that possesses a high binding affinity with ions [169]. An example of an ion-triggered drug release was reported by Lin *et al.* where they designed a phosphate-responsive DDS for the delivery of the anti-neoplastic drug cisplatin by the coordination of $–PO_3H_2$ (from phosphonoacetic acid) to the metal sites Zr^{4+} of UiO-66 [145]. Cisplatin molecules were incorporated into the modified UiO-66 *via* covalent conjugation with a loading efficiency of 25.7 wt.%. Cisplatin release was investigated *in vitro* in 10 mM PBS and 7.4 pH. The reported release, after 2 h, was 71%. The release mechanism could be attributed to the competitive coordination of phosphate, hydrogen phosphate, and dihydrogen phosphate ions from the PBS to the Zr_6 centers, causing the breakage of the MOF's structure and release of the therapeutic agent.

3.2.2. Exogenous Stimuli-responsive Drug Delivery

Exogenous stimuli-responsive DDSs employ stimuli that are applied outside the body, such as light, magnetic field, ultrasound, *etc*. These stimuli have a major advantage over their endogenous counterparts by offering a better spatiotemporal/dosage control of the drug release from the DDS. Another advantage is that drug release is often independent of the physiological conditions of the human body, minimizing variable results among different individuals. Using external stimuli allows us to start and stop the drug release by activating and deactivating the stimulus, the same way an on/off switch works. One of the drawbacks of this type of DDSs is the absence of autonomy, where drug release cannot be initiated or controlled without the external stimuli as opposed to the endogenous stimuli-responsive systems. In addition, the degree of external stimuli (e.g., light, magnetic field, or ultrasound) penetration into the body to reach the target cells and activate the drug release from the nanocarrier poses a significant challenge. In addition, with respect to the magnetic-responsive DDSs, the performance of the composite is dependent on the amount of the magnetic-sensitive particles incorporated into the MOF. Thus a large amount of the samples may be needed for the magnetic stimulus to trigger drug release [110].

3.2.2.1. Light-triggered Drug Release

Light-triggered drug release is widely investigated in stimuli-responsive DDSs design thanks to the controllability, non-invasiveness, and ease of operation it offers [119]. Light-responsive DDSs contain photosensitive molecules that, upon illumination, convert light (electromagnetic radiation) into a different form of energy, causing conformational changes or bond cleavage in the MOF's structure, which leads to drug release [185]. Drug delivery can be either in a single release (upon the disintegration of the DDS) or in multiple stages when the DDS acts as an on/off switch upon activation/deactivation of the light-stimulus [110]. Also, the photosensitive material utilized in the design of the DDSs can be either an organic ligand that is part of the building block of the MOF structure (e.g., porphyrin, azobenzene dicarboxylate, and indocyanine green) [154, 167, 186] or nanoparticles (NPs) that are incorporated into the MOF (e.g., silver/gold-based NPs, upconversion (NIR to visible light) nanoparticles (UCNP), *etc*.) [164, 187, 188]. In addition, the therapeutic strategies achieved by light-responsive DDSs can be categorized into either photodynamic therapy (PDT) and/or pho-

tothermal therapy (PTT). In PDT, the activation of photosensitizers leads to energy transfer to the target cell generating reactive oxygen species (ROS), which can induce cell apoptosis and cell necrosis in the target tissue [189]. In the case of PTT, the energy absorbed is converted into heat. When it comes to infections and cancerous tumors, elevated temperatures denature cell proteins, inhibit DNA replication (growth inhibition), and cause membrane rupture, killing the pathogens and cancer cells [189]. More importantly, for drug delivery purposes, elevated temperatures due to light irradiation cause the destabilization of the MOF's structure leading to drug release. An example of a light-responsive MOF-based DDS design was reported by Roth Stefaniak *et al.* [154]. They prepared an intelligent DDS based on a UiO-type MOF using the photosensitive ligand azobenzene dicarboxylate (AZB) for the light-responsive release of the anticancer drug Fluorouracil (5-FU). The MOF was further modified by an amine-functionalized polyethylene glycol ($PEG\text{-}NH_2$) coating *via* a post-synthetic modification route to enhance the aqueous stability, biocompatibility, and half-life of the drug-encapsulated MOF. Due to this unique modification, the modified UiO MOF exhibited good stability in the dark and released the drug upon structure degradation when irradiated with 340-nm UV light. However, it should be noted that UV light as a stimulus is not suitable in real applications due to its ionizing nature and hence bioincompatibility. For this reason, visible light or near-infrared (NIR) sources have been investigated as a stimulus in light-responsive DDSs. For example, Zeng *et al.* constructed NIR-responsive DDS consisting of gold nanorods (AuNR) as a core and porphyrinic MOF as the shell [155]. The drug Camptothecin (CPT) was encapsulated into the nanocomposite with a loading efficiency of more than 25%. After 24 hours, less than 10% of the encapsulated CPT was released, but the rate of release increased to around 30% when the NIR-stimulus was applied at a pH of 5.0 and 808 nm NIR laser. Furthermore, the DDS exhibited synergistic photodynamic and photothermal effects for damaging the cancer cell *in vitro* and hampering tumor growth *in vivo*.

3.2.2.2. Other Exogenous Stimuli for Drug Release

Other utilized stimuli used to trigger drug release from MOFbased DDSs include ultrasound (US), magnetic fields, and temperature. The US-triggered release consists of sound waves at frequencies above the hearing range of humans (>20 kHz). These non-invasive waves induce drug release from the DDS *via* thermomechanical effects generated by sound waves and acoustic cavitation phenomena [190]. This happens because the oscillatory growth and collapse of the microbubbles (cavities) formed near the nanocarrier interface induce high shear stresses capable of destabilizing the nanocarrier's structure, releasing the drug in the process. Also, the cavitation phenomenon was found to enhance vessel permeability, thereby increasing the cellular uptake of the drug [118]. In addition to cavitation (mechanical effects), ultrasound can induce hyperthermia, which is currently researched to induce drug delivery.

Magnetic-responsive DDSs offer an attractive option to targeted drug delivery. The use of a magnetic field allows guiding the DDS to a specific area (e.g., tissues, organs, *etc*.), offering more concentrated and targeted drug release, thereby enhancing the treatment efficacy [110]. Also, the conversion of magnetic energy to thermal energy provides an enhanced therapeutic effect by inducing tumor hyperthermia [189]. This type of MOF-based DDS is constructed either using a magnetic MOF [191, 192] or incorporating magnetic-sensitive NPs such as iron oxides NPs into the structure of the MOF *via* encapsulation (core-shell composites) [193-196]. Furthermore, thermal-responsive MOFs can be applied to trigger drug release from MOF-based DDSs, since higher temperatures lead to the destabilization of the MOF's structure and weak-

en the interaction between the MOF and the encapsulated cargo. Through implementing this strategy, Silva *et al.* fabricated a

thermal-responsive core-shell nanocomposite that consists of a gold NPs (AuNPs) core surrounded by ZIF-8 with an incorporated trivalent Terbium (Tb^{3+}) shell [156]. The nanocomposite was loaded with 5-FU and achieved controlled drug release at physiological temperatures. Light irradiation (at 514.5 nm and 700 mW cm^{-2}) was employed for thermally-triggered release; hence thermal-responsive MOF-based DDSs can be tentatively combined with light-responsive DDSs under the same classification.

3.2.3. Multistimuli-responsive Drug Delivery

Multistimuli-responsive DDSs refer to systems that utilize two or more triggering mechanisms to achieve targeted and controlled drug delivery. In order to improve the efficiency of drug delivery, DDSs are usually designed to respond to more than one stimulus, either of the same class (endogenous or exogenous) or a combination of endogenous/exogenous stimuli. An example of multi stimuli-responsive MOF-based DDSs, a pH/US-responsive nanocomposite, was designed by An *et al.* [168]. The DDS was fabricated by encapsulating S-Nitrosoglutathione (GSNO) and chlorin e6 (Ce6) into ZIF-8 and then coating it with the cytomembrane of a cancerous cell. According to their study, the DDS (dubbed GCZ@M) exhibited excellent biocompatibility, good retention in tumor tissue and provided a sustainable pH/US-triggered release of both GSNO and Ce6. The US-triggered release of GSNO and Ce6 into tumor cells leads to the release of nitric oxide (NO) gas from GSNO and ROS generation from Ce6, which react with each other, producing highly reactive $ONOO^-$ molecules that significantly increased anticancer effects. Also, the sonodynamic therapy (SDT) effects were enhanced due to the longer and effective tumor hypoxia relief realized by US.

Moreover, an interesting trend in multi stimuli-responsive DDSs is the incorporation of supramolecules such as cyclodextrins [197-199] and pillararenes [169, 170, 200, 201] that endow the MOF with useful host-guest features. For example, Wu *et al.* synthesized a triple-responsive UiO-66-NH_2 MOF-based DDS [97]. The UiO-66-NH_2 MOF was encapsulated with Fe_3O_4 NPS followed by surface modification with 1-(6-bromohexyl) pyridinium bromide (Py) and the loading of the anti-neoplastic agent 5-FU. The surface functionalization with Py allowed for the anchoring of carboxylate pillar [6]arene (WP6) *via* dynamic host-guest interactions. The WP6 molecules act as nanovalves that prevent the premature release of the loaded drug and grants the DDS the capability of targeted, multi stimuli-responsive drug release over a prolonged time period in response to pH changes, temperature variations, and competitive ions (Ca^{2+} and Zn^{2+}).

The combination of a magnetic field and other stimuli (e.g., light or pH) has also been reported [171, 172]. Sharma *et al.* synthesized magnetic MOF (MIL-88B) encapsulating the chemotherapy drug DOX and the photosensitizer methylene blue (MB) dye for the magnetic-guided chemotherapy and light-activated PDT [171]. Their findings showed that the therapeutic potential of the dual drug-loaded MOF was enhanced by the magnetically-targeted delivery to the cells. Moreover, the ability to guide the DDS toward a specific part of the body under magnetic-field control is opening the door to a new territory in DDSs design. Recently, Wang *et al.* designed a motile MOF that can act as self-propelled micro robot (MOFBOT) under a magnetic field to deliver drugs to specific targets in the body [172]. The MOFBOT was constructed as a coreshell structure from artificial bacterial flagella (ABF) with a helical microstructure and coated with biocompatible and pH-responsive ZIF-8. The researchers loaded the ZIF-8 matrix with the fluorescent rhodamine B (RhB) dye as a proof of concept; however, this approach will lead to new advancements in developing micro robotics for drug delivery applications.

3.3. Multifunctional MOFs as Theranostic Platforms

MOF-based theranostic platforms refer to systems that combine therapeutic and diagnostic functionalities in a single system. In essence, they are stimuli-responsive DDSs combined with diagnostic imaging capabilities. These systems promise various advantages such as better/faster diagnosis, imaging-guided drug delivery, and reduced side effects by enabling the real-time monitoring of drug release, which will provide a treatment tailored to the individual needs of the patients [202, 203]. The approach to design these platforms depends on the desired imaging technique (modality). For example, in magnetic resonance imaging (MRI), incorporation of magnetic-responsive material, either as part of the MOF's structure as a metal cluster (e.g., iron) [204] or by encapsulating magnetic NPs [23, 205], enables the platform to be used as contrast agents. Similarly, the incorporation of luminescent material in the MOF, either as ligands [24] or by encapsulating fluorescent molecules/NPs [206, 207], endow the platform with fluorescence imaging capabilities. Herein, some representative examples of recently developed MOF-based theranostic platforms are highlighted.

Recently, Mukherjee *et al.* prepared a nanocomposite based on MIL-53(Fe) for theranostic applications [208]. The platform was fabricated by conjugating UCNPs ($NaGdF_4$:Yb/Er) on the surface of MIL-53(Fe) and loading it with DOX. At the same time, folic acid (FA) was also conjugated to the surface of MIL-53(Fe) to enhance the targeted delivery of the nanocarrier. Drug release was studied in PBS (pH 7.4 and 5.2), and the nanocomposite achieved a 67.5% and 80% release after 48 hours at pH 7.4 and 5.2, respectively. Furthermore, the nanocomposite exhibited excellent biocompatibility, strong antitumor performance, and cancer-improved cellular uptake according to the cytotoxicity and intracellular uptake studies. Because of the presence of UCNPs, the nanoplatform demonstrated good fluorescence and magnetic characteristics, indicating that it can be used in fluorescence imaging-guided drug delivery and as an MRI contrast agent (T1 and T2 modes).

In another study, Zhang *et al.* designed a multimodal theranostic platform that can be implemented in MRI-guided chemotherapy and fluorescent imaging [95]. The nanoplatform was synthesized using Gadolinium (Gd) metal ions and 5-boronobenzene-1,3-dicarboxylic acid (BBDC) ligand and loaded with DOX with a loading efficiency of 43.2%. Further, to enhance the biocompatibility and improve the active targeting of tumor cells, the surface of the MOF was coated with glucose. The enhanced surface coating with glucose acted as a pH-responsive layer preventing premature leakage of DOX and allowing the gradual drug release in comparison to the uncoated one. The group also extended the design strategy by replacing Gd with Ytterbium (Yb). The MOF was also coated with glucose and demonstrated the pH-responsive release of DOX. The Yb-MOF-Glu MOF confirmed its ability as an efficient x-ray computerized tomography (CT) contrast agent, thanks to the high X-ray attenuation exhibited by Yb. As a demonstration, the group utilized Yb-MOF-Glu to create 3D-rendering CT images of the gastrointestinal tract.

Another imaging technique that can be exploited through MOF-based theranostic platforms is photoacoustic imaging (PAI). This technique utilizes the detection of sound waves generated upon light excitation of a material (photoacoustic effect). For instance, Zhang *et al.* reported curcumin-loaded MIL-100(Fe) for the construction of a theranostic platform that combines PAI functionality with dual chemo-photothermal therapy [209]. First, curcumin was loaded into MIL-100(Fe)*via* pore encapsulation (MC NP); then, the loaded MOF was coated with polydopamine-modified hyaluronic acid (HA-PDA)

to improve the biocompatibility and colloidal stability of the composite (MCH NP) under physiological conditions. Moreover, HA-PDA coating improved the targeted drug delivery due to the interaction between HA and the overexpressed receptors (CD44) on the surface of the cancerous cells. Furthermore, the addition of the HA-PDA coating enhanced the NIR absorption of the nanocomposite compared to MIL-100(Fe) and MC NPs, leading to higher photothermal conversion efficiency. This was demonstrated by the increase in the temperature of the solution containing MCH NPs (ΔT was 38.9 °C), which was higher than in the case of MIL-100(Fe) and MC NPs (ΔT was negligible and 25.2 °C, respectively). Besides, the presence of HA-PDA added photoacoustic capability to the nanoplatform, which enabled the PAI-guided chemo-photothermal therapy.

Moreover, a dual-modality (MRI and PAI) theranostic system for combined chemo-photothermal therapy was constructed by Chen *et al.via* merging Fe-based MOF with hollow mesoporous organosilica nanoparticles (HMONs) with a PDA interlayer [98]. The DOX (used for its therapeutic effect) and indocyanine green (ICG) (used for its photothermal therapy) were successfully loaded into the composite with an encapsulating capacity of 11.88%. The synthesis of the composite consisted of first preparing HMONs, followed by the surface modification with PDA to obtain HMONs-PDA. Then, Fe-based MOF was grown on the surface *via* the layer-by-layer deposition method, and finally, the formed composite was PEGylated using PEG-NH_2. DOX was loaded in the interior cavity of HMONs prior to the surface modification with PDA, while ICG was deposited on the outer surface of the composite after the PEGylation step. The loaded nanoplatform (dubbed DI@HMONs-PMOF) exhibited a pH/NIR stimuli-responsive drug release. Also, the platform showed the utility of a dual MRI and PAI functionality thanks to the Fe ions coordinated with PDA, as well as the ICG molecules on the MOF surface. Finally, the dual chemo-photothermal therapeutic efficiency was proven both *in vitro* and *in vivo*.

4. FUTURE OUTLOOK AND CHALLENGES

This review has shown the great potential of novel MOFs in biomedical applications, especially in drug delivery. Their attractive features such as large surface area, large pore volume, thermal and chemical stability, excellent loading capacities, and structural tunability led to the remarkable progress, witnessed in recent years, in the field of MOF-based DDSs and theranostic platforms. The current status of research and developments in relation to MOFbased biomedical devices promises an exciting future, where advanced systems that offer the capability of on-demand DDSs, self-regulated (autonomous) DDSs, micro-and nano-robotics will undoubtedly lead to substantial improvements in human healthcare.

Although remarkable developments have been made in MOFbased DDSs, significant hurdles and challenges still exist and must be tackled before moving to clinical trials. First, the biocompatibility of MOF-based DDSs is a major challenge that must be addressed. The *in vivo* short-term and long-term toxicity of MOFs needs to be investigated thoroughly. Their degradation mechanisms under physiological conditions must also be studied *in vivo*, starting from absorption, going through distribution, metabolism, and ending with excretion. Moreover, to aid in studying the degradation mechanism, the pharmacokinetic/pharmacodynamic behavior in the human body must be investigated and modeled. Another major challenge in the design of MOF-based DDSs is their colloidal/chemical stability. The design of the DDS must take into account the stability of the platform under physiological conditions. To enhance drug delivery efficacy, the DDS's physicochemical properties must be optimized to avoid aggregation and premature immune clearance, enhance blood circulation, and prevent premature drug release.

The synthesis of MOFs requires more environment-friendly methods. As discussed in the synthesis section, one of the most challenging aspects of synthesizing MOF is the selection of a safe and efficient solvent. Additionally, the synthesis methods must be selected to be implemented on a large scale while minimizing waste and maximizing yields. Finally, an essential aspect in constructing MOF-based DDSs is avoiding complex structural designs as much as possible since this may pose a challenge to batch preparation repeatability and future bulk synthesis. As a result, it leads to variations in the DDSs' performance.

CONCLUSION

In conclusion, this review presented a summary/discussion regarding the latest developments and advances in the field of MOFbased DDSs and theranostic platforms. The various methods utilized in MOF synthesis are summarized along with the advantages and disadvantages of each method. The MOF-based DDS preparation techniques are discussed, including preparation by incorporating the drug/biomolecule into the MOF's structure using surface adsorption, covalent conjugation, pore encapsulation, and *in situ* encapsulation or by directly applying the biomolecule as a ligand in the framework (bioMOF). MOFs' remarkable characteristics have led to a wide range of possible applications in biomedicine, including drug delivery. The MOF-based DDSs can be classified into normal (non-controllable) DDSs, stimuli-responsive DDSs, and theranostic platforms. The normal DDSs are pristine therapeutic agents loaded with therapeutic agents and offer little to no control over the drug release. Stimuli-responsive DDSs offer better spatiotemporal control over drug release by responding to either endogenous (pH, redox, ions, ATP) or exogenous stimuli (light, magnetism, US, pressure, temperature). The theranostic platforms combine stimuli-responsive drug delivery with diagnostic imaging functionality, paving the road for imaging-guided drug delivery. The reports summarized in this literature review (in terms of drug loading efficiencies and targeted/controlled release) promise a great future in the fight against diseases. However, numerous challenges must be addressed before moving to clinical applications.

CONSENT FOR PUBLICATION

Not applicable.

FUNDING

The authors gratefully acknowledge the financial support by the American University of Sharjah Enhanced Faculty Research grants (EFRG18-BBR-CEN-03 and FRG20-M-E84).

CONFLICT OF INTEREST

The authors declare that they have no conflict of interest.

ACKNOWLEDGEMENTS

The authors gratefully acknowledge the financial support by the American University of Sharjah.

REFERENCES

[1] Siegel, R.L.; Miller, K.D.; Jemal, A. Cancer statistics, 2019. *CA Cancer J.Clin.,* **2019**, *69*(1), 7-34.http://dx.doi.org/10.3322/caac.21551 PMID

[2] Ibrahim, M.; Sabouni, R.; Husseini, G.A. Anti-cancer Drug Delivery Using Metal Organic Frameworks (MOFs). *Curr. Med. Chem.,* **2017**, *24*(2), 193-214. http://dx.doi.org/10.2174/0929867323666160926151216 PMID: 27686655

[3] DeVita, V.T., Jr; Chu, E. A history of cancer chemotherapy. *Cancer Res.,* **2008**, *68*(21), 8643-8653. http://dx.doi.org/10.1158/0008-5472.CAN-07-6611 PMID: 18974103 Kayl, A.E.; Meyers, C.A. Side-effects of

[4] chemotherapy and quality of life in ovarian and breast cancer patients. *Curr. Opin. Obstet. Gynecol.,* **2006**, *18*(1), 24-28. http://dx.doi.org/10.1097/01.gco.0000192996.20040.24 PMID: 16493256 Li, Y.; Lu, A.; Long, M.; Cui, L.; Chen, Z.; Zhu, L. Nitroimidazole derivative

[5] incorporated liposomes for hypoxia-triggered drug delivery and enhanced therapeutic efficacy in patient-derived tumor xenografts. *Acta Biomater.,* **2019**, *83*, 334-348. http://dx.doi.org/10.1016/j.actbio.2018.10.029 PMID: 30366135 Mousavikhamene, Z.; Abdekhodaie, M.J.; Ahmadieh, H. Facilitation of transscleral

[6] drug delivery by drug loaded magnetic polymeric particles. *Mater. Sci. Eng. C,* **2017**, *79*, 812-820. http://dx.doi.org/10.1016/j.msec.2017.05.015 PMID: 28629084 Leong, J.; Chin, W.; Ke, X.; Gao, S.; Kong, H.; Hedrick, J.L.; Yang, Y.Y.

[7] Disease-directed design of biodegradable polymers: Reactive oxygen species and pH-responsive micellar nanoparticles for anticancer drug delivery. *Nanomedicine (Lond.),* **2018**, *14*(8), 2666-2677. http://dx.doi.org/10.1016/j.nano.2018.06.015 PMID: 30017961 Bai, Y.; Liu, C.P.; Song, X.; Zhuo, L.; Bu, H.; Tian, W. Photo- and pH- Dual-

[8] Responsive β-Cyclodextrin-Based Supramolecular Prodrug Complex Self-Assemblies for Programmed Drug Delivery. *Chem. Asian J.,* **2018**, *13*(24), 3903-3911. http://dx.doi.org/10.1002/asia.201801366 PMID: 30311448 Horcajada, P.; Serre, C.; Vallet-Regí, M.; Sebban, M.; Taulelle, F.; Férey, G.

[9] Metal-organic frameworks as efficient materials for drug delivery. *Angew. Chem. Int. Ed. Engl.,* **2006**, *45*(36), 5974-5978. http://dx.doi.org/10.1002/anie.200601878 PMID: 16897793

[10] Muñoz, B.; Rámila, A.; Pérez-Pariente, J.; Díaz, I.; Vallet-Regí, M. MCM-41 Organic Modification as Drug Delivery Rate Regulator. *Chem. Mater.,* **2003**, *15*(2), 500-503. http://dx.doi.org/10.1021/cm021217q

[11] El-Boubbou, K. Magnetic iron oxide nanoparticles as drug carriers: preparation, conjugation and delivery. *Nanomedicine (Lond.),* **2018**, *13*(8), 929-952. http://dx.doi.org/10.2217/nnm-2017-0320 PMID: 29546817 Kaluzova, M.; Bouras, A.; Machaidze, R.; Hadjipanayis, C.G. Targeted

[12] therapy of glioblastoma stem-like cells and tumor non-stem cells using cetuximab-conjugated iron-oxide nanoparticles. *Oncotarget,* **2015**, *6*(11), 8788-8806. http://dx.doi.org/10.18632/oncotarget.3554 PMID: 25871395 Pardo, J.; Peng, Z.; Leblanc, R.M. Cancer Targeting and Drug Delivery Using Carbon-Based Quantum Dots and Nanotubes. *Molecules,* **2018**, *23*(2),

[13] 378. http://dx.doi.org/10.3390/molecules23020378 PMID: 29439409 Cai, H.; Huang, Y-L.; Li, D. Biological Metal–Organic Frameworks: Structures, Host–Guest Chemistry and Bio-Applications. *Coord. Chem. Rev.,* **2019**, *378*, 207-221. http://dx.doi.org/10.1016/j.ccr.2017.12.003

[14] An, H.; Li, M.; Gao, J.; Zhang, Z.; Ma, S.; Chen, Y. Incorporation of Biomolecules in Metal-Organic Frameworks for Advanced Applications. *Coord. Chem. Rev.,* **2019**, *384*, 90-106. http://dx.doi.org/10.1016/j.ccr.2019.01.001

[15] Abánades Lázaro, I.; Forgan, R.S. Application of Zirconium MOFs in Drug Delivery and Biomedicine. *Coord. Chem. Rev.,* **2019**, *380*, 230-259. http://dx.doi.org/10.1016/j.ccr.2018.09.009 Zhang, Z.; Sang, W.; Xie, L.; Dai, Y. Metal-Organic Frameworks for Multimodal

[16] Bioimaging and Synergistic Cancer Chemotherapy. *Coord. Chem. Rev.,* **2019**, *399*, 213022. http://dx.doi.org/10.1016/j.ccr.2019.213022

[17] Wang, H-S. Metal–Organic Frameworks for Biosensing and Bioimaging Applications. *Coord. Chem. Rev.,* **2017**, *349*, 139-155. http://dx.doi.org/10.1016/j.ccr.2017.08.015

[18] Furukawa, H.; Cordova, K. E.; O'Keeffe, M.; Yaghi, O. M. The Chemistry and Applications of Metal-Organic Frameworks. *Science (80-.).,* **2013**, *341*(6149), 1230444-1230444. Farha, O.K.; Eryazici, I.; Jeong, N.C.; Hauser, B.G.; Wilmer, C.E.; Sarjeant,

[19] A.A.; Snurr, R.Q.; Nguyen, S.T.; Yazaydın, A.Ö.; Hupp, J.T. Metal-organic framework materials with ultrahigh surface areas: is the sky the limit? *J. Am. Chem. Soc.,* **2012**, *134*(36), 15016-15021. http://dx.doi.org/10.1021/ja3055639 PMID: 22906112 Furukawa, H.; Go, Y.B.; Ko, N.; Park, Y.K.; Uribe-Romo, F.J.; Kim, J.;

[20] O'Keeffe, M.; Yaghi, O.M. Isoreticular expansion of metal-organic frameworks with triangular and square building units and the lowest calculated density for porous crystals. *Inorg. Chem.,* **2011**, *50*(18), 9147-9152. http://dx.doi.org/10.1021/ic201376t PMID: 21842896 Aguilera-Sigalat, J.; Bradshaw, D. Synthesis and Applications of Metal-Organic

[21] Framework–Quantum Dot (QD@MOF) Composites. *Coord. Chem. Rev.,* **2016**, *307*, 267-291. http://dx.doi.org/10.1016/j.ccr.2015.08.004

[22] Yang, J-C.; Chen, Y.; Li, Y-H.; Yin, X-B. Magnetic Resonance Imaging-Guided Multi-Drug Chemotherapy and Photothermal Synergistic Therapy with pH and NIR-Stimulation Release. *ACS Appl. Mater. Interfaces,* **2017**, *9*(27), 22278-22288. http://dx.doi.org/10.1021/acsami.7b06105 PMID: 28616966

[23] Liu, W.; Wang, Y-M.; Li, Y-H.; Cai, S-J.; Yin, X-B.; He, X-W.; Zhang, YK. Fluorescent Imaging-Guided Chemotherapy-and-Photodynamic Dual Therapy with Nanoscale Porphyrin Metal-Organic Framework. *Small,* **2017**, *13*(17), 1603459. http://dx.doi.org/10.1002/smll.201603459 PMID: 28244202

[24] Yang, J.; Yang, Y.W. Metal-Organic Frameworks for Biomedical Applications. *Small,* **2020**, *16*(10), e1906846. http://dx.doi.org/10.1002/smll.201906846 PMID: 32026590

[25] Giliopoulos, D.; Zamboulis, A.; Giannakoudakis, D.; Bikiaris, D.; Triantafyllidis, K. Polymer/Metal Organic Framework (MOF) Nanocomposites for Biomedical Applications. *Molecules,* **2020**, *25*(1), 185. http://dx.doi.org/10.3390/molecules25010185 PMID: 31906398

[26] Chedid, G.; Yassin, A. Recent Trends in Covalent and Metal Organic Frameworks for Biomedical Applications. *Nanomaterials (Basel),* **2018**, *8*(11), 916. http://dx.doi.org/10.3390/nano8110916 PMID: 30405018

[27] Lu, K.; Aung, T.; Guo, N.; Weichselbaum, R.; Lin, W. Nanoscale Metal-Organic Frameworks for Therapeutic, Imaging, and Sensing Applications. *Adv. Mater.,* **2018**, *30*(37), e1707634. http://dx.doi.org/10.1002/adma.201707634 PMID: 29971835

[28] Wang, L.; Zheng, M.; Xie, Z. Nanoscale metal-organic frameworks for drug delivery: a conventional platform with new promise. *J. Mater. Chem. B Mater. Biol. Med.,* **2018**, *6*(5), 707-717. http://dx.doi.org/10.1039/C7TB02970E PMID: 32254257

[29] Liu, Y.; Zhao, Y.; Chen, X. Bioengineering of Metal-organic Frameworks for Nanomedicine. *Theranostics,* **2019**, *9*(11), 3122-3133. http://dx.doi.org/10.7150/thno.31918 PMID: 31244945

[30] Wang, Y.; Yan, J.; Wen, N.; Xiong, H.; Cai, S.; He, Q.; Hu, Y.; Peng, D.; Liu, Z.; Liu, Y. Metal-organic frameworks for stimuli-responsive drug delivery. *Biomaterials,* **2020**, *230*(230), 119619. http://dx.doi.org/10.1016/j.biomaterials.2019.119619 PMID: 31757529 Li, Y.; Li, X.; Guan, Q.; Zhang, C.; Xu, T.; Dong, Y.; Bai, X.; Zhang, W.

[31] Strategy for chemotherapeutic delivery using a nanosized porous metal-organic framework with a central composite design. *Int. J. Nanomedicine,* **2017**, *12*, 1465-1474. http://dx.doi.org/10.2147/IJN.S119115 PMID: 28260892

[32] Simon-Yarza, T.; Mielcarek, A.; Couvreur, P.; Serre, C. Nanoparticles of Metal-Organic Frameworks: On the Road to *In Vivo* Efficacy in Biomedicine. *Adv. Mater.,* **2018**, *30*(37), e1707365. http://dx.doi.org/10.1002/adma.201707365 PMID: 29876985

[33] Bahrani, S.; Hashemi, S.A.; Mousavi, S.M.; Azhdari, R. Zinc-based metal-organic frameworks as nontoxic and biodegradable platforms for biomedical applications: review study. *Drug Metab. Rev.,* **2019**, *51*(3), 356-377. http://dx.doi.org/10.1080/03602532.2019.1632887 PMID: 31203696 Mehta,

[34] J.; Bhardwaj, N.; Bhardwaj, S.K.; Kim, K-H.; Deep, A. Recent Advances in Enzyme Immobilization Techniques: Metal-Organic Frameworks as Novel Substrates. *Coord. Chem. Rev.,* **2016**, *322*, 30-40. http://dx.doi.org/10.1016/j.ccr.2016.05.007

[35] Chen, X-Y.; Zhao, B.; Shi, W.; Xia, J.; Cheng, P.; Liao, D-Z.; Yan, S-P.; Jiang, Z-H. Microporous Metal−Organic Frameworks Built on a Ln 3 Cluster as a Six-Connecting Node. *Chem. Mater.,* **2005**, *17*(11), 2866-2874. http://dx.doi.org/10.1021/cm050526o

[36] Wang, D.; He, H.; Chen, X.; Feng, S.; Niu, Y.; Sun, D. A 3D Porous Metal–Organic Framework Constructed of 1D Zigzag and Helical Chains Exhibiting Selective Anion Exchange. *CrystEngComm,* **2010**, *12*(4), 1041-1043. http://dx.doi.org/10.1039/B910988A

[37] Wu, J-Y.; Chao, T-C.; Zhong, M-S. Influence of Counteranions on the Structural Modulation of Silver–Di(3-Pyridylmethyl)Amine Coordination Polymers. *Cryst. Growth Des.,* **2013**, *13*(7), 2953-2964. http://dx.doi.org/10.1021/cg400363e

[38] Li, H.; Davis, C.E.; Groy, T.L.; Kelley, D.G.; Yaghi, O.M. Coordinatively Unsaturated Metal Centers in the Extended Porous Framework of Zn 3 (BDC) 3 ·6CH 3 OH (BDC = 1,4-Benzenedicarboxylate). *J. Am. Chem. Soc.,* **1998**, *120*(9), 2186-2187. http://dx.doi.org/10.1021/ja974172g

[39] Piñeiro-López, L.; Arcís-Castillo, Z.; Muñoz, M.C.; Real, J.A. Clathration of Five-Membered Aromatic Rings in the Bimetallic Spin Crossover Metal–Organic Framework [Fe(TPT) 2/3 {M I (CN) 2 } 2]·G (M I = Ag, Au). *Cryst. Growth Des.,* **2014**, *14*(12), 6311-6319. http://dx.doi.org/10.1021/cg5010616

[40] Shekhah, O.; Wang, H.; Kowarik, S.; Schreiber, F.; Paulus, M.; Tolan, M.; Sternemann, C.; Evers, F.; Zacher, D.; Fischer, R.A.; Wöll, C. Step-by-step route for the synthesis of metal-organic frameworks. *J. Am. Chem. Soc.,* **2007**, *129*(49), 15118-15119. http://dx.doi.org/10.1021/ja076210u PMID: 18020338

[41] Shekhah, O. Layer-by-Layer Method for the Synthesis and Growth of Sur

[42]

face Mounted Metal-Organic Frameworks (SURMOFs). *Materials (Basel),* **2010**, *3*(2), 1302-1315. http://dx.doi.org/10.3390/ma3021302

[43] Schoedel, A.; Scherb, C.; Bein, T. Oriented nanoscale films of metal-organic frameworks by room-temperature gel-layer synthesis. *Angew. Chem. Int. Ed. Engl.,* **2010**, *49*(40), 7225-7228. http://dx.doi.org/10.1002/anie.201001684 PMID: 20730844

[44] Lee, D-J.; Li, Q.; Kim, H.; Lee, K. Preparation of Ni-MOF-74 Membrane for CO2 Separation by Layer-by-Layer Seeding Technique. *Microporous Mesoporous Mater.,* **2012**, *163*, 169-177. http://dx.doi.org/10.1016/j.micromeso.2012.07.008

[45] Qiu, S.; Zhu, G. Molecular Engineering for Synthesizing Novel Structures of Metal–Organic Frameworks with Multifunctional Properties. *Coord. Chem. Rev.,* **2009**, *253*(23–24), 2891-2911. http://dx.doi.org/10.1016/j.ccr.2009.07.020

[46] Shen, L.; Wu, W.; Liang, R.; Lin, R.; Wu, L. Highly dispersed palladium nanoparticles anchored on UiO-66(NH_2) metal-organic framework as a reusable and dual functional visible-light-driven photocatalyst. *Nanoscale,* **2013**, *5*(19), 9374-9382. http://dx.doi.org/10.1039/c3nr03153e PMID: 23959004

[47] Serre, C.; Millange, F.; Thouvenot, C.; Noguès, M.; Marsolier, G.; Louër, D.; Férey, G. Very large breathing effect in the first nanoporous chromium(III)-based solids: MIL-53 or Cr(III)(OH) x [O(2)C-C(6)H(4)-CO(2)] x [HO(2)C-C(6)H(4)-CO(2)H](x) x H(2)O(y). *J. Am. Chem. Soc.,* **2002**, *124*(45), 13519-13526. http://dx.doi.org/10.1021/ja0276974 PMID: 12418906

[48] Zhang, Y.; Bo, X.; Nsabimana, A.; Han, C.; Li, M.; Guo, L. Electrocatalytically Active Cobalt-Based Metal–Organic Framework with Incorporated Macroporous Carbon Composite for Electrochemical Applications. *J. Mater. Chem. A Mater. Energy Sustain.,* **2015**, *3*(2), 732-738. http://dx.doi.org/10.1039/C4TA04411H

[49] Ni, Z.; Masel, R.I. Rapid production of metal-organic frameworks *via* microwave-assisted solvothermal synthesis. *J. Am. Chem. Soc.,* **2006**, *128*(38), 12394-12395. http://dx.doi.org/10.1021/ja0635231 PMID: 16984171

[50] Sabouni, R.; Kazemian, H.; Rohani, S. Microwave Synthesis of the CPM-5 Metal Organic Framework. *Chem. Eng. Technol.,* **2012**, *35*(6), 1085-1092. http://dx.doi.org/10.1002/ceat.201100626

[51] Stock, N.; Biswas, S. Synthesis of metal-organic frameworks (MOFs): routes to various MOF topologies, morphologies, and composites. *Chem. Rev.,* **2012**, *112*(2), 933-969. http://dx.doi.org/10.1021/cr200304e PMID: 22098087

[53] Morsali, A.; Monfared, H.H.; Morsali, A.; Janiak, C. Ultrasonic irradiation assisted syntheses of one-dimensional di(azido)-dipyridylamine Cu(II) coordination polymer nanoparticles. *Ultrason. Sonochem.,* **2015**, *23*, 208-211. http://dx.doi.org/10.1016/j.ultsonch.2014.06.005 PMID: 25164270

[54] Jung, D-W.; Yang, D-A.; Kim, J.; Kim, J.; Ahn, W-S. Facile synthesis of MOF-177 by a sonochemical method using 1-methyl-2-pyrrolidinone as a solvent. *Dalton Trans.,* **2010**, *39*(11), 2883-2887. http://dx.doi.org/10.1039/b925088c PMID: 20200716

[55] Jin, L-N.; Liu, Q.; Sun, W-Y. An Introduction to Synthesis and Application of Nanoscale Metal–Carboxylate Coordination Polymers. *CrystEngComm,* **2014**, *16*(19), 3816. http://dx.doi.org/10.1039/c3ce41962b

[56] Van Assche, T.R.C.; Desmet, G.; Ameloot, R.; De Vos, D.E.; Terryn, H.; Denayer, J.F.M. Electrochemical Synthesis of Thin HKUST-1 Layers on Copper Mesh. *Microporous Mesoporous Mater.,* **2012**, *158*, 209-213. http://dx.doi.org/10.1016/j.micromeso.2012.03.029

[57] Campagnol, N.; Souza, E.R.; De Vos, D.E.; Binnemans, K.; Fransaer, J. Luminescent terbium-containing metal-organic framework films: new approaches for the electrochemical synthesis and application as detectors for explosives. *Chem. Commun. (Camb.),* **2014**, *50*(83), 12545-12547. http://dx.doi.org/10.1039/C4CC05742B PMID: 25196133

[58] James, S.L.; Adams, C.J.; Bolm, C.; Braga, D.; Collier, P.; Friščić, T.; Grepioni, F.; Harris, K.D.M.; Hyett, G.; Jones, W.; Krebs, A.; Mack, J.; Maini, L.; Orpen, A.G.; Parkin, I.P.; Shearouse, W.C.; Steed, J.W.; Waddell, D.C. Mechanochemistry: opportunities for new and cleaner synthesis. *Chem. Soc. Rev.,* **2012**, *41*(1), 413-447. http://dx.doi.org/10.1039/C1CS15171A PMID: 21892512

[59] Masoomi, M.Y.; Morsali, A.; Junk, P.C. Rapid Mechanochemical Synthesis of Two New Cd(<scp>ii</Scp>)-Based Metal–Organic Frameworks with High Removal Efficiency of Congo Red. *CrystEngComm,* **2015**, *17*(3), 686-692. http://dx.doi.org/10.1039/C4CE01783H

[60] Ahnfeldt, T.; Guillou, N.; Gunzelmann, D.; Margiolaki, I.; Loiseau, T.; Férey, G.; Senker, J.; Stock, N. [Al4(OH)2(OCH3)4(H2N-bdc)3] x xH(2)O: a 12-connected porous metal-organic framework with an unprecedented aluminum-containing brick. *Angew. Chem. Int. Ed. Engl.,* **2009**, *48*(28), 5163-5166. http://dx.doi.org/10.1002/anie.200901409 PMID: 19504512

[61] Gani, R.; Jiménez-González, C.; Constable, D.J.C. Method for Selection of Solvents for Promotion of Organic Reactions. *Comput. Chem. Eng.,* **2005**, *29*(7), 1661-1676. http://dx.doi.org/10.1016/j.compchemeng.2005.02.021

[62] Li, P.; Cheng, F-F.; Xiong, W-W.; Zhang, Q. New Synthetic Strategies to Prepare Metal–Organic Frameworks. *Inorg. Chem. Front.,* **2018**, *5*(11), 2693-2708. http://dx.doi.org/10.1039/C8QI00543E

[63] Chen, J.; Wang, S-H.; Liu, Z-F.; Wu, M-F.; Xiao, Y.; Zheng, F-K.; Guo, GC.; Huang, J-S. Anion-Directed Self-Assembly of Cu(<scp>ii</Scp>) Coordination Compounds with Tetrazole-1-Acetic Acid: Syntheses in Ionic Liquids and Crystal Structures. *New J. Chem.,* **2014**, *38*(1), 269-276. http://dx.doi.org/10.1039/C3NJ01198D

[64] Yang, D-D.; Li, W.; Xiong, W-W.; Li, J-R.; Huang, X-Y. Ionothermal synthesis of discrete supertetrahedral Tn (n = 4, 5) clusters with tunable components, band gaps, and fluorescence properties. *Dalton Trans.,* **2018**, *47*(17), 5977-5984. http://dx.doi.org/10.1039/C8DT00524A PMID: 29589630

[65] Zhang, Q.; De Oliveira Vigier, K.; Royer, S.; Jérôme, F. Deep eutectic solvents: syntheses, properties and applications. *Chem. Soc. Rev.,* **2012**, *41*(21), 7108-7146. http://dx.doi.org/10.1039/c2cs35178a PMID: 22806597

[66] Francisco, M.; van den Bruinhorst, A.; Kroon, M.C. Low-transition-temperature mixtures (LTTMs): a new generation of designer solvents. *Angew. Chem. Int. Ed. Engl.,* **2013**, *52*(11), 3074-3085. http://dx.doi.org/10.1002/anie.201207548 PMID: 23401138

[67] Smith, E.L.; Abbott, A.P.; Ryder, K.S. Deep eutectic solvents (DESs) and their applications. *Chem. Rev.,* **2014**, *114*(21), 11060-11082. http://dx.doi.org/10.1021/cr300162p PMID: 25300631

[68] Yu, X.; Toh, Y.S.; Zhao, J.; Nie, L.; Ye, K.; Wang, Y.; Li, D.; Zhang, Q. Surfactant-Thermal Method to Prepare Two New Cobalt Metal-Organic Frameworks. *J. Solid State Chem.,* **2015**, *232*, 14-18. http://dx.doi.org/10.1016/j.jssc.2015.08.048

[69] Wang, S.; McGuirk, C.M.; d'Aquino, A.; Mason, J.A.; Mirkin, C.A. Metal-Organic Framework Nanoparticles. *Adv. Mater.,* **2018**, *30*(37), e1800202. http://dx.doi.org/10.1002/adma.201800202 PMID: 29862586

[70] Giménez-Marqués, M.; Hidalgo, T.; Serre, C.; Horcajada, P. Nanostructured Metal–Organic Frameworks and Their Bio-Related Applications. *Coord. Chem. Rev.,* **2016**, *307*, 342-360. http://dx.doi.org/10.1016/j.ccr.2015.08.008

[71] Peng, S.; Bie, B.; Sun, Y.; Liu, M.; Cong, H.; Zhou, W.; Xia, Y.; Tang, H.; Deng, H.; Zhou, X. Metal-organic frameworks for precise inclusion of single-stranded DNA and transfection in immune cells. *Nat. Commun.,* **2018**, *9*(1), 1293. http://dx.doi.org/10.1038/s41467-018-03650-w PMID: 29615605

[72] Sun, C-Y.; Qin, C.; Wang, X-L.; Su, Z-M. Metal-organic frameworks as potential drug delivery systems. *Expert Opin. Drug Deliv.,* **2013**, *10*(1), 89-101. http://dx.doi.org/10.1517/17425247.2013.741583 PMID: 23140545

[73] Abánades Lázaro, I.; Haddad, S.; Sacca, S.; Orellana-Tavra, C.; FairenJimenez, D.; Forgan, R.S. Selective Surface PEGylation of UiO-66 Nanoparticles for Enhanced Stability, Cell Uptake, and pH-Responsive Drug Delivery. *Chem,* **2017**, *2*(4), 561-578. http://dx.doi.org/10.1016/j.chempr.2017.02.005 PMID: 28516168

[74] Zhang, F-M.; Dong, H.; Zhang, X.; Sun, X-J.; Liu, M.; Yang, D-D.; Liu, X.; Wei, J-Z. Postsynthetic Modification of ZIF-90 for Potential Targeted Codelivery of Two Anticancer Drugs. *ACS Appl. Mater. Interfaces,* **2017**, *9*(32), 27332-27337. http://dx.doi.org/10.1021/acsami.7b08451 PMID: 28745483

[75] Liu, J.; Zhang, L.; Lei, J.; Shen, H.; Ju, H. Multifunctional Metal-Organic Framework Nanoprobe for Cathepsin B-Activated Cancer Cell Imaging and Chemo-Photodynamic Therapy. *ACS Appl. Mater. Interfaces,* **2017**, *9*(3), 2150-2158. http://dx.doi.org/10.1021/acsami.6b14446 PMID: 28033467

[76] Agostoni, V.; Horcajada, P.; Noiray, M.; Malanga, M.; Aykaç, A.; Jicsinszky, L.; Vargas-Berenguel, A.; Semiramoth, N.; Daoud-Mahammed, S.; Nicolas, V.; Martineau, C.; Taulelle, F.; Vigneron, J.; Etcheberry, A.; Serre, C.; Gref, R. A "green" strategy to construct non-covalent, stable and bioactive coatings on porous MOF nanoparticles. *Sci. Rep.,* **2015**, *5*(1), 7925. http://dx.doi.org/10.1038/srep07925 PMID: 25603994

[77] He, C.; Lu, K.; Liu, D.; Lin, W. Nanoscale metal-organic frameworks for the co-delivery of cisplatin and pooled siRNAs to enhance therapeutic efficacy in drug-resistant ovarian cancer cells. *J. Am. Chem. Soc.,* **2014**, *136*(14), 5181-5184. http://dx.doi.org/10.1021/ja4098862 PMID: 24669930

[78] Wang, C.; Gao, J.; Tan, H. Integrated Antibody with Catalytic Metal-Organic Framework for Colorimetric Immunoassay. *ACS Appl. Mater. Interfaces,* **2018**, *10*(30), 25113-25120. http://dx.doi.org/10.1021/acsami.8b07225 PMID: 29993238

[79] Lian, X.; Huang, Y.; Zhu, Y.; Fang, Y.; Zhao, R.; Joseph, E.; Li, J.; Pellois, J-P.; Zhou, H-C. Enzyme-MOF Nanoreactor Activates Nontoxic Paracetamol for Cancer Therapy. *Angew. Chem. Int. Ed. Engl.,* **2018**, *57*(20), 5725-5730. http://dx.doi.org/10.1002/anie.201801378 PMID: 29536600

Alizadeh, N.; Salimi, A.; Hallaj, R.; Fathi, F.; Soleimani, F. Ni-hemin metal-organic framework with highly efficient peroxidase catalytic activity: toward colorimetric cancer cell detection and targeted therapeutics. *J. Nano-*

[80] *biotechnology,* **2018**, *16*(1), 93. http://dx.doi.org/10.1186/s12951-018-0421-7 PMID: 30458781

[81] Liu, X.; Yan, Z.; Zhang, Y.; Liu, Z.; Sun, Y.; Ren, J.; Qu, X. Two-Dimensional Metal-Organic Framework/Enzyme Hybrid Nanocatalyst as a Benign and Self-Activated Cascade Reagent for *in Vivo* Wound Healing. *ACS Nano,* **2019**, *13*(5), 5222-5230. http://dx.doi.org/10.1021/acsnano.8b09501 PMID: 31002497

[82] Wu, X.; Ge, J.; Yang, C.; Hou, M.; Liu, Z. Facile synthesis of multiple enzyme-containing metal-organic frameworks in a biomolecule-friendly environment. *Chem. Commun. (Camb.),* **2015**, *51*(69), 13408-13411. http://dx.doi.org/10.1039/C5CC05136C PMID: 26214658

[83] Mohammad, M.; Razmjou, A.; Liang, K.; Asadnia, M.; Chen, V. Metal-Organic-Framework-Based Enzymatic Microfluidic Biosensor *via* Surface Patterning and Biomineralization. *ACS Appl. Mater. Interfaces,* **2019**, *11*(2), 1807-1820. http://dx.doi.org/10.1021/acsami.8b16837 PMID: 30525376

[84] Liu, X.; Qi, W.; Wang, Y.; Lin, D.; Yang, X.; Su, R.; He, Z. Rational Design of Mimic Multienzyme Systems in Hierarchically Porous Biomimetic Metal-Organic Frameworks. *ACS Appl. Mater. Interfaces,* **2018**, *10*(39), 33407-33415. http://dx.doi.org/10.1021/acsami.8b09388 PMID: 30146872

[85] Xu, W.; Jiao, L.; Yan, H.; Wu, Y.; Chen, L.; Gu, W.; Du, D.; Lin, Y.; Zhu, C. Glucose Oxidase-Integrated Metal-Organic Framework Hybrids as Biomimetic Cascade Nanozymes for Ultrasensitive Glucose Biosensing. *ACS Appl. Mater. Interfaces,* **2019**, *11*(25), 22096-22101. http://dx.doi.org/10.1021/acsami.9b03004 PMID: 31134797

[86] Ning, D.; Liu, Q.; Wang, Q.; Du, X-M.; Ruan, W-J.; Li, Y. Luminescent MOF Nanosheets for Enzyme Assisted Detection of H2O2 and Glucose and Activity Assay of Glucose Oxidase. *Sens. Actuators B Chem.,* **2019**, *282*, 443-448. http://dx.doi.org/10.1016/j.snb.2018.11.088

[87] Yin, Y.; Gao, C.; Xiao, Q.; Lin, G.; Lin, Z.; Cai, Z.; Yang, H. Protein-Metal Organic Framework Hybrid Composites with Intrinsic Peroxidase-like Activity as a Colorimetric Biosensing Platform. *ACS Appl. Mater. Interfaces,* **2016**, *8*(42), 29052-29061. http://dx.doi.org/10.1021/acsami.6b09893 PMID: 27700042

[88] Hu, Y.; Cheng, H.; Zhao, X.; Wu, J.; Muhammad, F.; Lin, S.; He, J.; Zhou, L.; Zhang, C.; Deng, Y.; Wang, P.; Zhou, Z.; Nie, S.; Wei, H. Surface-Enhanced Raman Scattering Active Gold Nanoparticles with Enzyme-Mimicking Activities for Measuring Glucose and Lactate in Living Tissues. *ACS Nano,* **2017**, *11*(6), 5558-5566. http://dx.doi.org/10.1021/acsnano.7b00905 PMID: 28549217

[89] Xu, R.; Wang, Y.; Duan, X.; Lu, K.; Micheroni, D.; Hu, A.; Lin, W. Nanoscale Metal-Organic Frameworks for Ratiometric Oxygen Sensing in Live Cells. *J. Am. Chem. Soc.,* **2016**, *138*(7), 2158-2161. http://dx.doi.org/10.1021/jacs.5b13458 PMID: 26864385

[90] Zhang, X.; Fang, L.; Jiang, K.; He, H.; Yang, Y.; Cui, Y.; Li, B.; Qian, G. Nanoscale fluorescent metal-organic framework composites as a logic platform for potential diagnosis of asthma. *Biosens. Bioelectron.,* **2019**, *130*, 65-72. http://dx.doi.org/10.1016/j.bios.2019.01.011 PMID: 30731347

[91] Liu, C-S.; Zhang, Z-H.; Chen, M.; Zhao, H.; Duan, F-H.; Chen, D-M.; Wang, M-H.; Zhang, S.; Du, M. Pore modulation of zirconium-organic frameworks for high-efficiency detection of trace proteins. *Chem. Commun. (Camb.),* **2017**, *53*(28), 3941-3944. http://dx.doi.org/10.1039/C7CC00029D PMID: 28300246

[92] Deng, J.; Wang, K.; Wang, M.; Yu, P.; Mao, L. Mitochondria Targeted Nanoscale Zeolitic Imidazole Framework-90 for ATP Imaging in Live Cells. *J. Am. Chem. Soc.,* **2017**, *139*(16), 5877-5882. http://dx.doi.org/10.1021/jacs.7b01229 PMID: 28385016

[93] Yang, C.; Chen, K.; Chen, M.; Hu, X.; Huan, S-Y.; Chen, L.; Song, G.; Zhang, X-B. Nanoscale Metal-Organic Framework Based Two-Photon Sensing Platform for Bioimaging in Live Tissue. *Anal. Chem.,* **2019**, *91*(4), 2727-2733. http://dx.doi.org/10.1021/acs.analchem.8b04405 PMID: 30663316

[94] Robison, L.; Zhang, L.; Drout, R.J.; Li, P.; Haney, C.R.; Brikha, A.; Noh, H.; Mehdi, B.L.; Browning, N.D.; Dravid, V.P. A Bismuth Metal–Organic Framework as a Contrast Agent for X-Ray Computed Tomography. *ACS Appl. Bio Mater.,* **2019**, *2*(3), 1197-1203. http://dx.doi.org/10.1021/acsabm.8b00778

[95] Sene, S.; Marcos-Almaraz, M.T.; Menguy, N.; Scola, J.; Volatron, J.; Rouland, R.; Grenèche, J-M.; Miraux, S.; Menet, C.; Guillou, N. Maghemite-NanoMIL-100(Fe) Bimodal Nanovector as a Platform for Image-Guided Therapy. *Chem,* **2017**, *3*(2), 303-322. http://dx.doi.org/10.1016/j.chempr.2017.06.007

[96] Zhang, H.; Shang, Y.; Li, Y-H.; Sun, S-K.; Yin, X-B. Smart Metal-Organic Framework-Based Nanoplatforms for Imaging-Guided Precise Chemotherapy. *ACS Appl. Mater. Interfaces,* **2019**, *11*(2), 1886-1895. http://dx.doi.org/10.1021/acsami.8b19048 PMID: 30584757

[97] Shang, W.; Zeng, C.; Du, Y.; Hui, H.; Liang, X.; Chi, C.; Wang, K.; Wang, Z.; Tian, J. Core-Shell Gold Nanorod@Metal-Organic Framework Nanoprobes for Multimodality Diagnosis of Glioma. *Adv. Mater.,* **2017**, *29*(3), 1604381. http://dx.doi.org/10.1002/adma.201604381 PMID: 27859713

[97] Wu, M-X.; Gao, J.; Wang, F.; Yang, J.; Song, N.; Jin, X.; Mi, P.; Tian, J.; Luo, J.; Liang, F.; Yang, Y.W. Multistimuli Responsive Core-Shell Nanoplatform Constructed from Fe_3O_4 @MOF Equipped with Pillar[6]arene Nanovalves. *Small,* **2018**, *14*(17), e1704440. http://dx.doi.org/10.1002/smll.201704440 PMID: 29611291

[98] Chen, L.; Zhang, J.; Zhou, X.; Yang, S.; Zhang, Q.; Wang, W.; You, Z.; Peng, C.; He, C. Merging metal organic framework with hollow organosilica nanoparticles as a versatile nanoplatform for cancer theranostics. *Acta Biomater.,* **2019**, *86*, 406-415. http://dx.doi.org/10.1016/j.actbio.2019.01.005 PMID: 30625415

[99] Lin, J.; Xin, P.; An, L.; Xu, Y.; Tao, C.; Tian, Q.; Zhou, Z.; Hu, B.; Yang, S. Fe_3O_4-ZIF-8 assemblies as pH and glutathione responsive T_2-T_1 switching magnetic resonance imaging contrast agent for sensitive tumor imaging *in vivo*. *Chem. Commun. (Camb.),* **2019**, *55*(4), 478-481. http://dx.doi.org/10.1039/C8CC08943D PMID: 30547169

[100] Sava Gallis, D.F.; Butler, K.S.; Agola, J.O.; Pearce, C.J.; McBride, A.A. Antibacterial Countermeasures *via* Metal-Organic Framework-Supported Sustained Therapeutic Release. *ACS Appl. Mater. Interfaces,* **2019**, *11*(8), 7782-7791. http://dx.doi.org/10.1021/acsami.8b21698 PMID: 30682243

[101] Berchel, M.; Le Gall, T.; Denis, C.; Le Hir, S.; Quentel, F.; Elléouet, C.; Montier, T.; Rueff, J-M.; Salaün, J-Y.; Haelters, J-P. A Silver-Based Metal–Organic Framework Material as a 'Reservoir' of Bactericidal Metal Ions. *New J. Chem.,* **2011**, *35*(5), 1000. http://dx.doi.org/10.1039/c1nj20202b

[102] Chiericatti, C.; Basilico, J.C.; Zapata Basilico, M.L.; Zamaro, J.M. Novel Application of HKUST-1 Metal–Organic Framework as Antifungal: Biological Tests and Physicochemical Characterizations. *Microporous Mesoporous Mater.,* **2012**, *162*, 60-63. http://dx.doi.org/10.1016/j.micromeso.2012.06.012

[103] Li, P.; Li, J.; Feng, X.; Li, J.; Hao, Y.; Zhang, J.; Wang, H.; Yin, A.; Zhou, J.; Ma, X.; Wang, B. Metal-organic frameworks with photocatalytic bactericidal activity for integrated air cleaning. *Nat. Commun.,* **2019**, *10*(1), 2177. http://dx.doi.org/10.1038/s41467-019-10218-9 PMID: 31097709

[104] Lin, S.; Liu, X.; Tan, L.; Cui, Z.; Yang, X.; Yeung, K.W.K.; Pan, H.; Wu, S. Porous Iron-Carboxylate Metal-Organic Framework: A Novel Bioplatform with Sustained Antibacterial Efficacy and Nontoxicity. *ACS Appl. Mater. Interfaces,* **2017**, *9*(22), 19248-19257. http://dx.doi.org/10.1021/acsami.7b04810 PMID: 28558188

[105] Zhang, Y.; Sun, P.; Zhang, L.; Wang, Z.; Wang, F.; Dong, K.; Liu, Z.; Ren, J.; Qu, X. Silver-Infused Porphyrinic Metal-Organic Framework: Surface-Adaptive, On-Demand Nanoplatform for Synergistic Bacteria Killing and Wound Disinfection. *Adv. Funct. Mater.,* **2019**, *29*(11), 1808594. http://dx.doi.org/10.1002/adfm.201808594

[106] Mao, D.; Hu, F.; Kenry; Ji, S.; Wu, W.; Ding, D.; Kong, D.; Liu, B. Metal-Organic-Framework-Assisted *In Vivo* Bacterial Metabolic Labeling and Precise Antibacterial Therapy. *Adv. Mater.,* **2018**, *30*(18), e1706831. http://dx.doi.org/10.1002/adma.201706831 PMID: 29504163

[107] Chen, H.; Yang, J.; Sun, L.; Zhang, H.; Guo, Y.; Qu, J.; Jiang, W.; Chen, W.; Ji, J.; Yang, Y.W.; Wang, B. Synergistic Chemotherapy and Photodynamic Therapy of Endophthalmitis Mediated by Zeolitic Imidazolate Framework-Based Drug Delivery Systems. *Small,* **2019**, *15*(47), e1903880. http://dx.doi.org/10.1002/smll.201903880 PMID: 31588682

[108] Shakya, S.; He, Y.; Ren, X.; Guo, T.; Maharjan, A.; Luo, T.; Wang, T.; Dhakhwa, R.; Regmi, B.; Li, H.; Gref, R.; Zhang, J. Ultrafine Silver Nanoparticles Embedded in Cyclodextrin Metal-Organic Frameworks with GRGDS Functionalization to Promote Antibacterial and Wound Healing Application. *Small,* **2019**, *15*(27), e1901065. http://dx.doi.org/10.1002/smll.201901065 PMID: 31069948

[109] Soomro, N.A.; Wu, Q.; Amur, S.A.; Liang, H.; Ur Rahman, A.; Yuan, Q.; Wei, Y. Natural drug physcion encapsulated zeolitic imidazolate framework, and their application as antimicrobial agent. *Colloids Surf. B Biointerfaces,* **2019**, *182*, 110364. http://dx.doi.org/10.1016/j.colsurfb.2019.110364 PMID: 31352254

[110] Carrillo-Carrión, C. Nanoscale metal-organic frameworks as key players in the context of drug delivery: evolution toward theranostic platforms. *Anal. Bioanal. Chem.,* **2020**, *412*(1), 37-54. http://dx.doi.org/10.1007/s00216-019-02217-y PMID: 31734711

[111] Leng, X.; Dong, X.; Wang, W.; Sai, N.; Yang, C.; You, L.; Huang, H.; Yin, X.; Ni, J. Biocompatible Fe-Based Micropore Metal-Organic Frameworks as Sustained-Release Anticancer Drug Carriers. *Molecules,* **2018**, *23*(10), 2490. http://dx.doi.org/10.3390/molecules23102490 PMID: 30274195

[112] Liang, S.; Wu, X-L.; Xiong, J.; Zong, M-H.; Lou, W-Y. Metal-Organic Frameworks as Novel Matrices for Efficient Enzyme Immobilization: An Update Review. *Coord. Chem. Rev.,* **2020**, *406*, 213149. http://dx.doi.org/10.1016/j.ccr.2019.213149

[113] Taylor-Pashow, K.M.L.; Della Rocca, J.; Xie, Z.; Tran, S.; Lin, W. Postsynthetic modifications of iron-carboxylate nanoscale metal-organic frameworks for imaging and drug delivery. *J. Am. Chem. Soc.,* **2009**, *131*(40), 14261-14263. http://dx.doi.org/10.1021/ja906198y PMID: 19807179

[114] Wuttke, S.; Braig, S.; Preiß, T.; Zimpel, A.; Sicklinger, J.; Bellomo, C.; Rädler, J.O.; Vollmar, A.M.; Bein, T. MOF nanoparticles coated by lipid bi-

layers and their uptake by cancer cells. *Chem. Commun. (Camb.),* **2015**, *51*(87), 15752-15755.
http://dx.doi.org/10.1039/C5CC06767G PMID: 26359316

[115] Yang, J.; Chen, X.; Li, Y.; Zhuang, Q.; Liu, P.; Gu, J. Zr-Based MOFs Shielded with Phospholipid Bilayers: Improved Biostability and Cell Uptake for Biological Applications. *Chem. Mater.,* **2017**, *29*(10), 4580-4589. http://dx.doi.org/10.1021/acs.chemmater.7b01329

[116] Illes, B.; Hirschle, P.; Barnert, S.; Cauda, V.; Wuttke, S.; Engelke, H. Exosome-Coated Metal–Organic Framework Nanoparticles: An Efficient Drug Delivery Platform. *Chem. Mater.,* **2017**, *29*(19), 8042-8046. http://dx.doi.org/10.1021/acs.chemmater.7b02358

[117] Illes, B.; Wuttke, S.; Engelke, H. Liposome-Coated Iron Fumarate Metal-Organic Framework Nanoparticles for Combination Therapy. *Nanomaterials (Basel),* **2017**, *7*(11), 351.
http://dx.doi.org/10.3390/nano7110351 PMID: 29072630

[118] Mura, S.; Nicolas, J.; Couvreur, P. Stimuli-responsive nanocarriers for drug delivery. *Nat. Mater.,* **2013**, *12*(11), 991-1003.
http://dx.doi.org/10.1038/nmat3776 PMID: 24150417

[119] Jhaveri, A.; Deshpande, P.; Torchilin, V. Stimuli-sensitive nanopreparations for combination cancer therapy. *J. Control. Release,* **2014**, *190*, 352-370. http://dx.doi.org/10.1016/j.jconrel.2014.05.002 PMID: 24818767

[120] Tan, G.; Zhong, Y.; Yang, L.; Jiang, Y.; Liu, J.; Ren, F. A Multifunctional MOF-Based Nanohybrid as Injectable Implant Platform for Drug Synergistic Oral Cancer Therapy. *Chem. Eng. J.,* **2020**, *390*(February), 124446. http://dx.doi.org/10.1016/j.cej.2020.124446

[121] Liu, Z.; Wu, Q.; He, J.; Vriesekoop, F.; Liang, H. Crystal-Seeded Growth of PH-Responsive Metal–Organic Frameworks for Enhancing Encapsulation, Stability, and Bioactivity of Hydrophobicity Compounds. *ACS Biomater. Sci. Eng.,* **2019**, *5*(12), 6581-6589.
http://dx.doi.org/10.1021/acsbiomaterials.9b01070

[122] Javanbakht, S.; Pooresmaeil, M.; Namazi, H. Green one-pot synthesis of carboxymethylcellulose/Zn-based metal-organic framework/graphene oxide bio-nanocomposite as a nanocarrier for drug delivery system. *Carbohydr. Polym.,* **2019**, *208*, 294-301.
http://dx.doi.org/10.1016/j.carbpol.2018.12.066 PMID: 30658803

[123] Lv, Y.; Ding, D.; Zhuang, Y.; Feng, Y.; Shi, J.; Zhang, H.; Zhou, T-L.; Chen, H.; Xie, R-J. Chromium-Doped Zinc Gallogermanate@Zeolitic Imidazolate Framework-8: A Multifunctional Nanoplatform for Rechargeable *In Vivo* Persistent Luminescence Imaging and pH-Responsive Drug Release. *ACS Appl. Mater. Interfaces,* **2019**, *11*(2), 1907-1916. http://dx.doi.org/10.1021/acsami.8b19172 PMID: 30566326

[124] Liu, Y.; Zhang, C.; Liu, H.; Li, Y.; Xu, Z.; Li, L.; Whittaker, A. Controllable Synthesis of Up-Conversion Nanoparticles UCNPs@MIL-PEG for PH-Responsive Drug Delivery and Potential up-Conversion Luminescence/Magnetic Resonance Dual-Mode Imaging. *J. Alloys Compd.,* **2018**, *749*, 939-947.
http://dx.doi.org/10.1016/j.jallcom.2018.03.355

[125] Jiang, Z.; Yuan, B.; Qiu, N.; Wang, Y.; Sun, L.; Wei, Z.; Li, Y.; Zheng, J.; Jin, Y.; Li, Y. Manganese-Zeolitic Imidazolate Frameworks-90 with High Blood Circulation Stability for MRI-Guided Tumor Therapy. *Nano-Micro Lett.,* **2019**, *11*(1), 61.
http://dx.doi.org/10.1007/s40820-019-0292-y

[126] Qin, Y-T.; Peng, H.; He, X-W.; Li, W-Y.; Zhang, Y-K. pH-Responsive Polymer-Stabilized ZIF-8 Nanocomposites for Fluorescence and Magnetic Resonance Dual-Modal Imaging-Guided Chemo-/Photodynamic Combinational Cancer Therapy. *ACS Appl. Mater. Interfaces,* **2019**, *11*(37), 34268-34281.
http://dx.doi.org/10.1021/acsami.9b12641 PMID: 31454217

[127] Yang, Y.; Xu, L.; Zhu, W.; Feng, L.; Liu, J.; Chen, Q.; Dong, Z.; Zhao, J.; Liu, Z.; Chen, M. One-pot synthesis of pH-responsive charge-switchable PEGylated nanoscale coordination polymers for improved cancer therapy. *Biomaterials,* **2018**, *156*, 121-133.
http://dx.doi.org/10.1016/j.biomaterials.2017.11.038 PMID: 29195181

[128] Feng, J.; Xu, Z.; Dong, P.; Yu, W.; Liu, F.; Jiang, Q.; Wang, F.; Liu, X. Stimuli-responsive multifunctional metal-organic framework nanoparticles for enhanced chemo-photothermal therapy. *J. Mater. Chem. B Mater. Biol. Med.,* **2019**, *7*(6), 994-1004.
http://dx.doi.org/10.1039/C8TB02815J PMID: 32255104

[129] Zheng, C.; Wang, Y.; Phua, S.Z.F.; Lim, W.Q.; Zhao, Y. ZnO–DOX@ZIF-8 Core–Shell Nanoparticles for PH-Responsive Drug Delivery. *ACS Biomater. Sci. Eng.,* **2017**, *3*(10), 2223-2229.
http://dx.doi.org/10.1021/acsbiomaterials.7b00435

[130] Xue, Z.; Zhu, M.; Dong, Y.; Feng, T.; Chen, Z.; Feng, Y.; Shan, Z.; Xu, J.; Meng, S. An integrated targeting drug delivery system based on the hybridization of graphdiyne and MOFs for visualized cancer therapy. *Nanoscale,* **2019**, *11*(24), 11709-11718.
http://dx.doi.org/10.1039/C9NR02017A PMID: 31180099

[131] Nezhad-Mokhtari, P.; Arsalani, N.; Javanbakht, S.; Shaabani, A. Development of Gelatin Microsphere Encapsulated Cu-Based Metal-Organic Framework Nanohybrid for the Methotrexate Delivery. *J. Drug Deliv. Sci. Technol.,* **2019**, *50*, 174-180.
http://dx.doi.org/10.1016/j.jddst.2019.01.020

[132] Guo, Y.; Yan, B.; Cheng, Y.; Mu, L. A New Dy(III)-Based Metal-Organic

[133]

[134]

[135]

[136]

[137]

[138]

[139]

[140]

[141]

[142]

[143]

[144]

[145]

[146]

[147]

[148]

[149]

[150] Framework Nanoparticles (NMOFs) for the Controlled Release of Loads and Drugs. *Adv. Funct. Mater.,* **2017**, *27*(37), 1702102. http://dx.doi.org/10.1002/adfm.201702102

[151] Yang, X.; Tang, Q.; Jiang, Y.; Zhang, M.; Wang, M.; Mao, L. Nanoscale ATP-Responsive Zeolitic Imidazole Framework-90 as a General Platform for Cytosolic Protein Delivery and Genome Editing. *J. Am. Chem. Soc.,* **2019**, *141*(9), 3782-3786. http://dx.doi.org/10.1021/jacs.8b11996 PMID: 30722666

[152] Kim, K.; Lee, S.; Jin, E.; Palanikumar, L.; Lee, J.H.; Kim, J.C.; Nam, J.S.; Jana, B.; Kwon, T-H.; Kwak, S.K.; Choe, W.; Ryu, J.H. MOF × Biopolymer: Collaborative Combination of Metal-Organic Framework and Biopolymer for Advanced Anticancer Therapy. *ACS Appl. Mater. Interfaces,* **2019**, *11*(31), 27512-27520. http://dx.doi.org/10.1021/acsami.9b05736 PMID: 31293157

[153] Sun, Q.; Bi, H.; Wang, Z.; Li, C.; Wang, X.; Xu, J.; Zhu, H.; Zhao, R.; He, F.; Gai, S.; Yang, P. Hyaluronic acid-targeted and pH-responsive drug delivery system based on metal-organic frameworks for efficient antitumor therapy. *Biomaterials,* **2019**, *223*, 119473. http://dx.doi.org/10.1016/j.biomaterials.2019.119473 PMID: 31499255

[154] Lei, B.; Wang, M.; Jiang, Z.; Qi, W.; Su, R.; He, Z. Constructing Redox-Responsive Metal-Organic Framework Nanocarriers for Anticancer Drug Delivery. *ACS Appl. Mater. Interfaces,* **2018**, *10*(19), 16698-16706. http://dx.doi.org/10.1021/acsami.7b19693 PMID: 29692177

[155] Roth Stefaniak, K.; Epley, C.C.; Novak, J.J.; McAndrew, M.L.; Cornell, H.D.; Zhu, J.; McDaniel, D.K.; Davis, J.L.; Allen, I.C.; Morris, A.J.; Grove, T.Z. Photo-triggered release of 5-fluorouracil from a MOF drug delivery vehicle. *Chem. Commun. (Camb.),* **2018**, *54*(55), 7617-7620. http://dx.doi.org/10.1039/C8CC01601A PMID: 29926872

[156] Zeng, J-Y.; Zhang, M-K.; Peng, M-Y.; Gong, D.; Zhang, X-Z. Porphyrinic Metal-Organic Frameworks Coated Gold Nanorods as a Versatile Nanoplatform for Combined Photodynamic/Photothermal/Chemotherapy of Tumor. *Adv. Funct. Mater.,* **2018**, *28*(8), 1705451. http://dx.doi.org/10.1002/adfm.201705451

[157] Silva, J.Y.R.; Proenza, Y.G.; da Luz, L.L.; de Sousa Araújo, S.; Filho, M.A.G.; Junior, S.A.; Soares, T.A.; Longo, R.L. A thermo-responsive adsorbent-heater-thermometer nanomaterial for controlled drug release: (ZIF-8,Eu_xTb_y)@AuNP core-shell. *Mater. Sci. Eng. C,* **2019**, *102*, 578-588. http://dx.doi.org/10.1016/j.msec.2019.04.078 PMID: 31147030

[158] Adhikari, C.; Mishra, A.; Nayak, D.; Chakraborty, A. Metal Organic Frameworks Modified Mesoporous Silica Nanoparticles (MSN): A Nano-Composite System to Inhibit Uncontrolled Chemotherapeutic Drug Delivery from Bare-MSN. *J. Drug Deliv. Sci. Technol.,* **2018**, *47*, 1-11. http://dx.doi.org/10.1016/j.jddst.2018.06.015

[159] Ren, S-Z.; Zhu, D.; Zhu, X-H.; Wang, B.; Yang, Y-S.; Sun, W-X.; Wang, X-M.; Lv, P-C.; Wang, Z-C.; Zhu, H-L. Nanoscale Metal-Organic-Frameworks Coated by Biodegradable Organosilica for pH and Redox Dual Responsive Drug Release and High-Performance Anticancer Therapy. *ACS Appl. Mater. Interfaces,* **2019**, *11*(23), 20678-20688. http://dx.doi.org/10.1021/acsami.9b04236 PMID: 31081332

[160] Wu, M-X.; Yan, H-J.; Gao, J.; Cheng, Y.; Yang, J.; Wu, J-R.; Gong, B-J.; Zhang, H-Y.; Yang, Y-W. Multifunctional Supramolecular Materials Constructed from Polypyrrole@UiO-66 Nanohybrids and Pillararene Nanovalves for Targeted Chemophotothermal Therapy. *ACS Appl. Mater. Interfaces,* **2018**, *10*(40), 34655-34663. http://dx.doi.org/10.1021/acsami.8b13758 PMID: 30226739

[161] Lin, W.; Cui, Y.; Yang, Y.; Hu, Q.; Qian, G. A biocompatible metal-organic framework as a pH and temperature dual-responsive drug carrier. *Dalton Trans.,* **2018**, *47*(44), 15882-15887. http://dx.doi.org/10.1039/C8DT03202E PMID: 30362496

[162] Xing, K.; Fan, R.; Wang, F.; Nie, H.; Du, X.; Gai, S.; Wang, P.; Yang, Y. Dual-Stimulus-Triggered Programmable Drug Release and Luminescent Ratiometric pH Sensing from Chemically Stable Biocompatible Zinc Metal-Organic Framework. *ACS Appl. Mater. Interfaces,* **2018**, *10*(26), 22746-22756. http://dx.doi.org/10.1021/acsami.8b06270 PMID: 29877692

[163] Lin, W.; Hu, Q.; Jiang, K.; Cui, Y.; Yang, Y.; Qian, G. A Porous Zn-Based Metal-Organic Framework for PH and Temperature Dual-Responsive Controlled Drug Release. *Microporous Mesoporous Mater.,* **2017**, *249*, 55-60. http://dx.doi.org/10.1016/j.micromeso.2017.04.042

[164] Yang, C.; Xu, J.; Yang, D.; Wang, X.; Liu, B.; He, N.; Wang, Z. ICG@ZIF-8: One-Step Encapsulation of Indocyanine Green in ZIF-8 and Use as a Therapeutic Nanoplatform. *Chin. Chem. Lett.,* **2018**, *29*(9), 1421-1424. http://dx.doi.org/10.1016/j.cclet.2018.02.014

[165] Yang, X.; Li, L.; He, D.; Hai, L.; Tang, J.; Li, H.; He, X.; Wang, K. A metal-organic framework based nanocomposite with co-encapsulation of Pd@Au nanoparticles and doxorubicin for pH- and NIR-triggered synergistic chemo-photothermal treatment of cancer cells. *J. Mater. Chem. B Mater. Biol. Med.,* **2017**, *5*(24), 4648-4659. http://dx.doi.org/10.1039/C7TB00715A PMID: 32264307

Li, S.; Zhang, L.; Liang, X.; Wang, T.; Chen, X.; Liu, C.; Li, L.; Wang, C. Tailored Synthesis of Hollow MOF/Polydopamine Janus Nanoparticles for Synergistic Multi-Drug Chemo-Photothermal Therapy. *Chem. Eng. J.,* **2019**, *378*(February), 122175. http://dx.doi.org/10.1016/j.cej.2019.122175

[166] Tian, Z.; Yao, X.; Ma, K.; Niu, X.; Grothe, J.; Xu, Q.; Liu, L.; Kaskel, S.; Zhu, Y. Metal-Organic Framework/Graphene Quantum Dot Nanoparticles Used for Synergistic Chemo- and Photothermal Therapy. *ACS Omega,* **2017**, *2*(3), 1249-1258. http://dx.doi.org/10.1021/acsomega.6b00385 PMID: 30023630

[167] Luo, Z.; Jiang, L.; Yang, S.; Li, Z.; Soh, W.M.W.; Zheng, L.; Loh, X.J.; Wu, Y.L. Light-Induced Redox-Responsive Smart Drug Delivery System by Using Selenium-Containing Polymer@MOF Shell/Core Nanocomposite. *Adv. Healthc. Mater.,* **2019**, *8*(15), e1900406. http://dx.doi.org/10.1002/adhm.201900406 PMID: 31183979

[168] An, J.; Hu, Y-G.; Li, C.; Hou, X-L.; Cheng, K.; Zhang, B.; Zhang, R-Y.; Li, D-Y.; Liu, S-J.; Liu, B.; Zhu, D.; Zhao, Y.D. A pH/Ultrasound dual-response biomimetic nanoplatform for nitric oxide gas-sonodynamic combined therapy and repeated ultrasound for relieving hypoxia. *Biomaterials,* **2020**, *230*, 119636. http://dx.doi.org/10.1016/j.biomaterials.2019.119636 PMID: 31785776

[169] Tan, L-L.; Li, H.; Zhou, Y.; Zhang, Y.; Feng, X.; Wang, B.; Yang, Y-W. Zn(2+)-Triggered Drug Release from Biocompatible Zirconium MOFs Equipped with Supramolecular Gates. *Small,* **2015**, *11*(31), 3807-3813. http://dx.doi.org/10.1002/smll.201500155 PMID: 25919865

[170] Tan, L-L.; Song, N.; Zhang, S.X-A.; Li, H.; Wang, B.; Yang, Y-W. Ca^{2+}, pH and thermo triple-responsive mechanized Zr-based MOFs for on-command drug release in bone diseases. *J. Mater. Chem. B Mater. Biol. Med.,* **2016**, *4*(1), 135-140. http://dx.doi.org/10.1039/C5TB01789K PMID: 32262817

[171] Sharma, S.; Sethi, K.; Roy, I. Magnetic Nanoscale Metal–Organic Frameworks for Magnetically Aided Drug Delivery and Photodynamic Therapy. *New J. Chem.,* **2017**, *41*(20), 11860-11866. http://dx.doi.org/10.1039/C7NJ02032E

[172] Wang, X.; Chen, X.Z.; Alcântara, C.C.J.; Sevim, S.; Hoop, M.; Terzopoulou, A.; de Marco, C.; Hu, C.; de Mello, A.J.; Falcaro, P.; Furukawa, S.; Nelson, B.J.; Puigmartí-Luis, J.; Pané, S. MOFBOTS: Metal-Organic-Framework-Based Biomedical Microrobots. *Adv. Mater.,* **2019**, *31*(27), e1901592. http://dx.doi.org/10.1002/adma.201901592 PMID: 31058366

[173] Dai, Y.; Xu, C.; Sun, X.; Chen, X. Nanoparticle design strategies for enhanced anticancer therapy by exploiting the tumour microenvironment. *Chem. Soc. Rev.,* **2017**, *46*(12), 3830-3852. http://dx.doi.org/10.1039/C6CS00592F PMID: 28516983

[174] Gupta, V.; Tyagi, S.; Paul, A.K. Development of Biocompatible Iron-Carboxylate Metal Organic Frameworks for pH-Responsive Drug Delivery Application. *J. Nanosci. Nanotechnol.,* **2019**, *19*(2), 646-654. http://dx.doi.org/10.1166/jnn.2019.15402 PMID: 30360136

[175] Chen, W-H.; Yu, X.; Cecconello, A.; Sohn, Y.S.; Nechushtai, R.; Willner, I. Stimuli-responsive nucleic acid-functionalized metal-organic framework nanoparticles using pH- and metal-ion-dependent DNAzymes as locks. *Chem. Sci. (Camb.),* **2017**, *8*(8), 5769-5780. http://dx.doi.org/10.1039/C7SC01765K PMID: 28989617

[176] Guan, X.; Guo, Z.; Wang, T.; Lin, L.; Chen, J.; Tian, H.; Chen, X. A pH-Responsive Detachable PEG Shielding Strategy for Gene Delivery System in Cancer Therapy. *Biomacromolecules,* **2017**, *18*(4), 1342-1349. http://dx.doi.org/10.1021/acs.biomac.7b00080 PMID: 28272873

[177] Kanamala, M.; Wilson, W.R.; Yang, M.; Palmer, B.D.; Wu, Z. Mechanisms and biomaterials in pH-responsive tumour targeted drug delivery: A review. *Biomaterials,* **2016**, *85*, 152-167. http://dx.doi.org/10.1016/j.biomaterials.2016.01.061 PMID: 26871891

[178] Karakeçili, A.; Topuz, B.; Korpayev, S.; Erdek, M. Metal-organic frameworks for on-demand pH controlled delivery of vancomycin from chitosan scaffolds. *Mater. Sci. Eng. C,* **2019**, *105*, 110098. http://dx.doi.org/10.1016/j.msec.2019.110098 PMID: 31546383

[179] Cabrera-García, A.; Checa-Chavarria, E.; Rivero-Buceta, E.; Moreno, V.; Fernández, E.; Botella, P. Amino modified metal-organic frameworks as pH-responsive nanoplatforms for safe delivery of camptothecin. *J. Colloid Interface Sci.,* **2019**, *541*, 163-174. http://dx.doi.org/10.1016/j.jcis.2019.01.042 PMID: 30685611

[180] Liu, W.; Zhong, Y.; Wang, X.; Zhuang, C.; Chen, J.; Liu, D.; Xiao, W.; Pan, Y.; Huang, J.; Liu, J. A Porous Cu(II)-Based Metal-Organic Framework Carrier for PH-Controlled Anticancer Drug Delivery. *Inorg. Chem. Commun.,* **2020**, *111*, 107675. http://dx.doi.org/10.1016/j.inoche.2019.107675

[181] Jhaveri, A.M.; Torchilin, V.P. Multifunctional polymeric micelles for delivery of drugs and siRNA. *Front. Pharmacol.,* **2014**, *5*, 77. http://dx.doi.org/10.3389/fphar.2014.00077 PMID: 24795633

[182] Liu, Y.; Gong, C.S.; Dai, Y.; Yang, Z.; Yu, G.; Liu, Y.; Zhang, M.; Lin, L.; Tang, W.; Zhou, Z.; Zhu, G.; Chen, J.; Jacobson, O.; Kiesewetter, D.O.; Wang, Z.; Chen, X. In situ polymerization on nanoscale metal-organic frameworks for enhanced physiological stability and stimulus-responsive intracellular drug delivery. *Biomaterials,* **2019**, *218*, 119365. http://dx.doi.org/10.1016/j.biomaterials.2019.119365 PMID: 31344642

[183] Xue, Q.; Ye, C.; Zhang, M.; Hu, X.; Cai, T. Glutathione responsive cubic gel particles cyclodextrin metal-organic frameworks for intracellular drug delivery. *J. Colloid Interface Sci.,* **2019**, *551*, 39-46. http://dx.doi.org/10.1016/j.jcis.2019.04.096 PMID: 31075632

[184]

Drug Deliv., **2016**, *13*(3), 311-314. http://dx.doi.org/10.1517/17425247.2016.1140147 PMID: 26745457

[185] Rwei, A.Y.; Wang, W.; Kohane, D.S. Photoresponsive nanoparticles for drug delivery. *Nano Today,* **2015**, *10*(4), 451-467. http://dx.doi.org/10.1016/j.nantod.2015.06.004 PMID: 26644797

[186] Jiang, K.; Zhang, L.; Hu, Q.; Yue, D.; Zhang, J.; Zhang, X.; Li, B.; Cui, Y.; Yang, Y.; Qian, G. Indocyanine Green–Encapsulated Nanoscale Metal–Organic Frameworks for Highly Effective Chemo-Photothermal Combination Cancer Therapy. *Mater. Today Nano,* **2018**, *2*, 50-57. http://dx.doi.org/10.1016/j.mtnano.2018.09.001

[187] Xu, X-Y.; Chu, C.; Fu, H.; Du, X-D.; Wang, P.; Zheng, W.; Wang, C-C. Light-Responsive UiO-66-NH2/Ag3PO4 MOF-Nanoparticle Composites for the Capture and Release of Sulfamethoxazole. *Chem. Eng. J.,* **2018**, *350*, 436-444. http://dx.doi.org/10.1016/j.cej.2018.06.005

[188] Cai, H-J.; Shen, T-T.; Zhang, J.; Shan, C-F.; Jia, J-G.; Li, X.; Liu, W-S.; Tang, Y. A core-shell metal-organic-framework (MOF)-based smart nanocomposite for efficient NIR/H_2O_2-responsive photodynamic therapy against hypoxic tumor cells. *J. Mater. Chem. B Mater. Biol. Med.,* **2017**, *5*(13), 2390-2394. http://dx.doi.org/10.1039/C7TB00314E PMID: 32264545

[189] Yao, J.; Feng, J.; Chen, J. External-Stimuli Responsive Systems for Cancer Theranostic. *Asian J. Pharm. Sci.,* **2016**, *11*(5), 585-595. http://dx.doi.org/10.1016/j.ajps.2016.06.001

[190] Tanbour, R.; Martins, A.M.; Pitt, W.G.; Husseini, G.A. Drug Delivery Systems Based on Polymeric Micelles and Ultrasound: A Review. *Curr. Pharm. Des.,* **2016**, *22*(19), 2796-2807. http://dx.doi.org/10.2174/1381612822666160217125215 PMID: 26898742

[191] Terzopoulou, A.; Hoop, M.; Chen, X.Z.; Hirt, A.M.; Charilaou, M.; Shen, Y.; Mushtaq, F.; Del Pino, A.P.; Logofatu, C.; Simonelli, L.; de Mello, A.J.; Doonan, C.J.; Sort, J.; Nelson, B.J.; Pané, S.; Puigmartí-Luis, J. Mineralization-Inspired Synthesis of Magnetic Zeolitic Imidazole Framework Composites. *Angew. Chem. Int. Ed. Engl.,* **2019**, *58*(38), 13550-13555. http://dx.doi.org/10.1002/anie.201907389 PMID: 31309662

[192] Sethi, K.; Sharma, S.; Roy, I. Nanoscale Iron Carboxylate Metal Organic Frameworks as Drug Carriers for Magnetically Aided Intracellular Delivery. *RSC Advances,* **2016**, *6*(80), 76861-76866. http://dx.doi.org/10.1039/C6RA18480D

[193] Wu, Y.N.; Zhou, M.; Li, S.; Li, Z.; Li, J.; Wu, B.; Li, G.; Li, F.; Guan, X. Magnetic metal-organic frameworks: γ-Fe2O3@MOFs *via* confined in situ pyrolysis method for drug delivery. *Small,* **2014**, *10*(14), 2927-2936. http://dx.doi.org/10.1002/smll.201400362 PMID: 24644065

[194] Wang, D.; Zhou, J.; Chen, R.; Shi, R.; Xia, G.; Zhou, S.; Liu, Z.; Zhang, N.; Wang, H.; Guo, Z.; Chen, Q. Magnetically guided delivery of DHA and Fe ions for enhanced cancer therapy based on pH-responsive degradation of DHA-loaded Fe3O4@C@MIL-100(Fe) nanoparticles. *Biomaterials,* **2016**, *107*, 88-101. http://dx.doi.org/10.1016/j.biomaterials.2016.08.039 PMID: 27614161

[195] Li, S.; Bi, K.; Xiao, L.; Shi, X. Facile preparation of magnetic metal organic frameworks core-shell nanoparticles for stimuli-responsive drug carrier. *Nanotechnology,* **2017**, *28*(49), 495601. http://dx.doi.org/10.1088/1361-6528/aa91c4 PMID: 28985188

[196] Tovar, M.A.; Parkhurst, A.; Matuczinski, E.; Balenger, S.; Giancarlo, L.C. Synthesis of a superparamagnetic iron oxide based nano-complex for targeted cell death of glioblastoma cells. *Nanotechnology,* **2019**, *30*(46), 465101. http://dx.doi.org/10.1088/1361-6528/ab33d4 PMID: 31323657

[197] Abuçafy, M.P.; Caetano, B.L.; Chiari-Andréo, B.G.; Fonseca-Santos, B.; do Santos, A.M.; Chorilli, M.; Chiavacci, L.A. Supramolecular cyclodextrin-based metal-organic frameworks as efficient carrier for anti-inflammatory drugs. *Eur. J. Pharm. Biopharm.,* **2018**, *127*, 112-119. http://dx.doi.org/10.1016/j.ejpb.2018.02.009 PMID: 29428794

[198]

[199] Singh, V.; Guo, T.; Wu, L.; Xu, J.; Liu, B.; Gref, R.; Zhang, J. Template-Directed Synthesis of a Cubic Cyclodextrin Polymer with Aligned Channels and Enhanced Drug Payload. *RSC Advances,* **2017**, *7*(34), 20789-20794. http://dx.doi.org/10.1039/C7RA02306E

[200] Sha, J-Q.; Zhong, X-H.; Wu, L-H.; Liu, G-D.; Sheng, N. Nontoxic and Renewable Metal–Organic Framework Based on α-Cyclodextrin with Efficient Drug Delivery. *RSC Advances,* **2016**, *6*(86), 82977-82983. http://dx.doi.org/10.1039/C6RA16549D

[201] Tan, L-L.; Li, H.; Qiu, Y-C.; Chen, D-X.; Wang, X.; Pan, R-Y.; Wang, Y.; Zhang, S.X-A.; Wang, B.; Yang, Y-W. Stimuli-responsive metal-organic frameworks gated by pillar[5]arene supramolecular switches. *Chem. Sci. (Camb.),* **2015**, *6*(3), 1640-1644. http://dx.doi.org/10.1039/C4SC03749A PMID: 30154997

[202] Yang, K.; Yang, K.; Chao, S.; Wen, J.; Pei, Y.; Pei, Z. A supramolecular hybrid material constructed from pillar[6]arene-based host-guest complexation and ZIF-8 for targeted drug delivery. *Chem. Commun. (Camb.),* **2018**, *54*(70), 9817-9820. http://dx.doi.org/10.1039/C8CC05665J PMID: 30109320

[203] Jo, S.D.; Ku, S.H.; Won, Y-Y.; Kim, S.H.; Kwon, I.C. Targeted Nanotheranostics for Future Personalized Medicine: Recent Progress in Cancer Therapy. *Theranostics,* **2016**, *6*(9), 1362-1377. http://dx.doi.org/10.7150/thno.15335 PMID: 27375785

[204] He, L.; Liu, Y.; Lau, J.; Fan, W.; Li, Q.; Zhang, C.; Huang, P.; Chen, X. Recent progress in nanoscale metal-organic frameworks for drug release and cancer therapy. *Nanomedicine (Lond.),* **2019**, *14*(10), 1343-1365. http://dx.doi.org/10.2217/nnm-2018-0347 PMID: 31084393

[205] Horcajada, P.; Chalati, T.; Serre, C.; Gillet, B.; Sebrie, C.; Baati, T.; Eubank, J.F.; Heurtaux, D.; Clayette, P.; Kreuz, C.; Chang, J.S.; Hwang, Y.K.; Marsaud, V.; Bories, P.N.; Cynober, L.; Gil, S.; Férey, G.; Couvreur, P.; Gref, R. Porous metal-organic-framework nanoscale carriers as a potential platform for drug delivery and imaging. *Nat. Mater.,* **2010**, *9*(2), 172-178. http://dx.doi.org/10.1038/nmat2608 PMID: 20010827

[206] Zhao, H-X.; Zou, Q.; Sun, S-K.; Yu, C.; Zhang, X.; Li, R-J.; Fu, Y-Y. Theranostic metal-organic framework core-shell composites for magnetic resonance imaging and drug delivery. *Chem. Sci. (Camb.),* **2016**, *7*(8), 5294-5301. http://dx.doi.org/10.1039/C6SC01359G PMID: 30155180

[207] Cai, W.; Gao, H.; Chu, C.; Wang, X.; Wang, J.; Zhang, P.; Lin, G.; Li, W.; Liu, G.; Chen, X. Engineering Phototheranostic Nanoscale Metal-Organic Frameworks for Multimodal Imaging-Guided Cancer Therapy. *ACS Appl. Mater. Interfaces,* **2017**, *9*(3), 2040-2051. http://dx.doi.org/10.1021/acsami.6b11579 PMID: 28032505

[208] He, L.; Wang, T.; An, J.; Li, X.; Zhang, L.; Li, L.; Li, G.; Wu, X.; Su, Z.; Wang, C. Carbon Nanodots@zeolitic Imidazolate Framework-8 Nanoparticles for Simultaneous PH-Responsive Drug Delivery and Fluorescence Imaging. *CrystEngComm,* **2014**, *16*(16), 3259. http://dx.doi.org/10.1039/c3ce42506a

[209] Mukherjee, P.; Kumar, A.; Bhamidipati, K.; Puvvada, N.; Sahu, S.K. Facile Strategy to Synthesize Magnetic Upconversion Nanoscale Metal–Organic Framework Composites for Theranostics Application. *ACS Appl. Bio Mater.,* **2020**, *3*(2), 869-880. http://dx.doi.org/10.1021/acsabm.9b00949

Zhang, Y.; Wang, L.; Liu, L.; Lin, L.; Liu, F.; Xie, Z.; Tian, H.; Chen, X. Engineering Metal-Organic Frameworks for Photoacoustic Imaging-Guided Chemo-/Photothermal Combinational Tumor Therapy. *ACS Appl. Mater. Interfaces,* **2018**, *10*(48), 41035-41045. http://dx.doi.org/10.1021/acsami.8b13492 PMID: 30403471